Response to S. Solomon

First, we would like to thank Prof. Solomon for her insightful comments and suggestions. They have all been taken into account and they have allowed improving the paper. Each of the comments is addressed on a point-by-point basis hereafter, with the original comment reproduced in blue first.

1) There is a lot of discussion of the apparent onset of denitrification and its association with a 'threshold' T<195K. I think the paper would be stronger if this were accompanied by a discussion of the uncertainties in the temperatures used to identify this relationship (i.e., ERA-interim). Three questions arise a) Could it really be 194K within uncertainties? Why or why not? How sharp is this threshold within uncertainties? b) what about the influence of small scale waves that may not be resolved by the reanalysis? c) would there be value in simply doing a scatter plot of local HNO3 versus local temperature in winter, as opposed to the current approach of binning by eqlat?

We agree with the referee that the temperature of 195 K for the formation of PSCs can vary, namely depending on the conditions of the atmosphere, and that small scale waves would likely influence the local formation of PSCs. We plotted, as suggested by the referee, the HNO_3 values versus the temperature for each grid cell between 70 and 90°S of equivalent latitude for the winter months (May to October, see Figure here below). The appearance of low HNO_3 values occurs as expected around the 195 K threshold (red line), albeit with some variability, namely between 190 and 200 K. These variations are of interest when studying the precise dynamics of PSC formation and the results below suggest that IASI could make a strong contribution in monitoring the processes at play. We thank the referee for having triggered us to look into this in more details; we believe a forthcoming work could be undertaken regarding this question. However, for the present study, we believe that an average temperature of 195 K is a reasonable value to work with. We have mentioned these potential temperature variations in the text: *"It should be noted that while this temperature is a widely accepted approximation for the formation threshold for NAT (type I), its actual value can be different depending on the local conditions (Lowe and MacKenzie, 2008; Drdla and Müller, 2010; Hoyle et al., 2013)."* (p. 4, line 16-18)

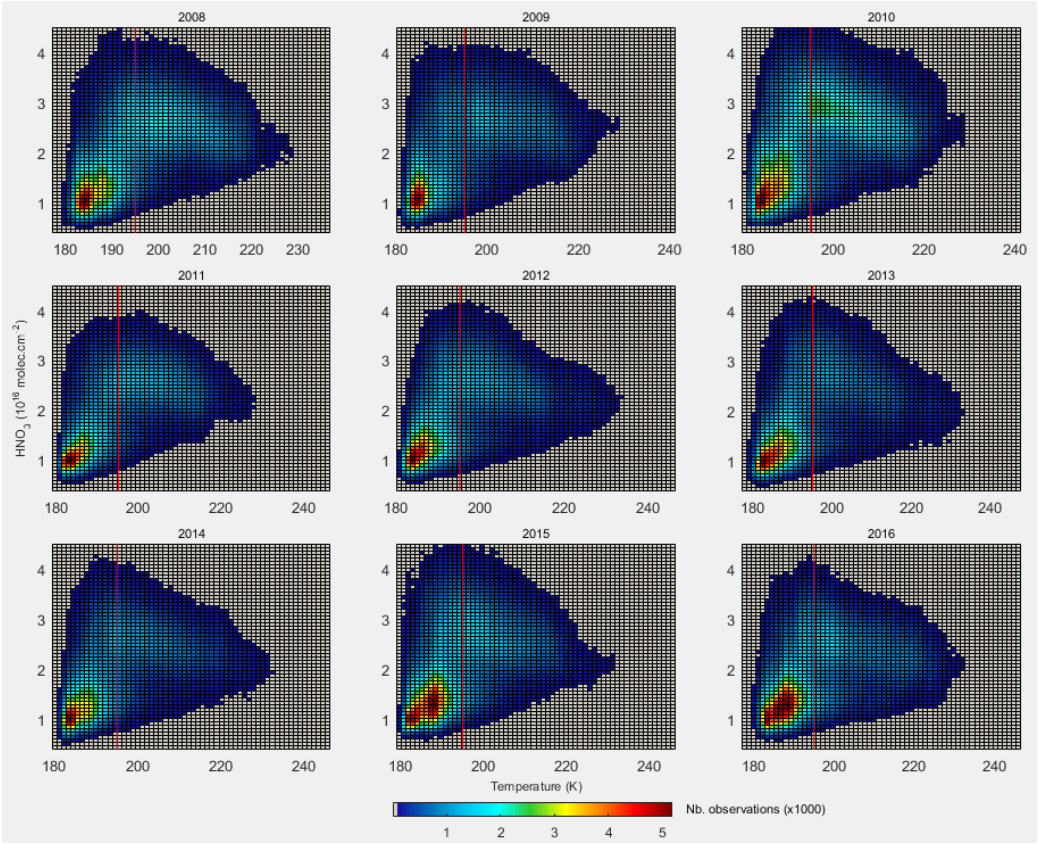

Figure 1. Total columns of HNO_3 (10^{16} molec.cm^{-2}) versus temperatures (K) for the 70-90 S eqlat band, and between May and October. The color scale indicates the number of measurements per bin (with grey areas for bins with less than 80 measurements), and the red line is the 195 K threshold.

2) Figures, 2, 3, and 4 are key results of this study, showing very well the seasonal cycles in the two hemispheres. A minor comment on Fig 2 is that heavy tics are needed for January, so one can see the exact mapping in time more readily.

We thank the reviewer for the positive feedback on the Figures. The ticks have been changed and they are now heavier for the months of January. This indeed makes the reading of the figure easier.

A substantive comment is that the time lag for recovery of the HNO3 column in the southern hemisphere is striking. The paper has some good discussion on this but I wonder if more could be done. In particular, if the mechanism replacing the HNO3 is mainly via transport, then HNO3 and O3 would show very similar post-final warming increases – do they? This could be shown, and would make the paper more useful.

We would like to thank Prof. Solomon for this useful comment. The behaviour of O_3 (retrieved from the same IASI observation) was compared against that of HNO_3, as shown with the Figure below. It appears that the recovery of O_3 at the end of the winter happens much sooner than that of HNO_3 (see Figure below). Note that the O_3 columns are stratospheric columns. We agree with the referee that this is a good indication that the mechanism for HNO_3 recovery is not due to transport and mixing but more with chemistry, as addressed in the next point.

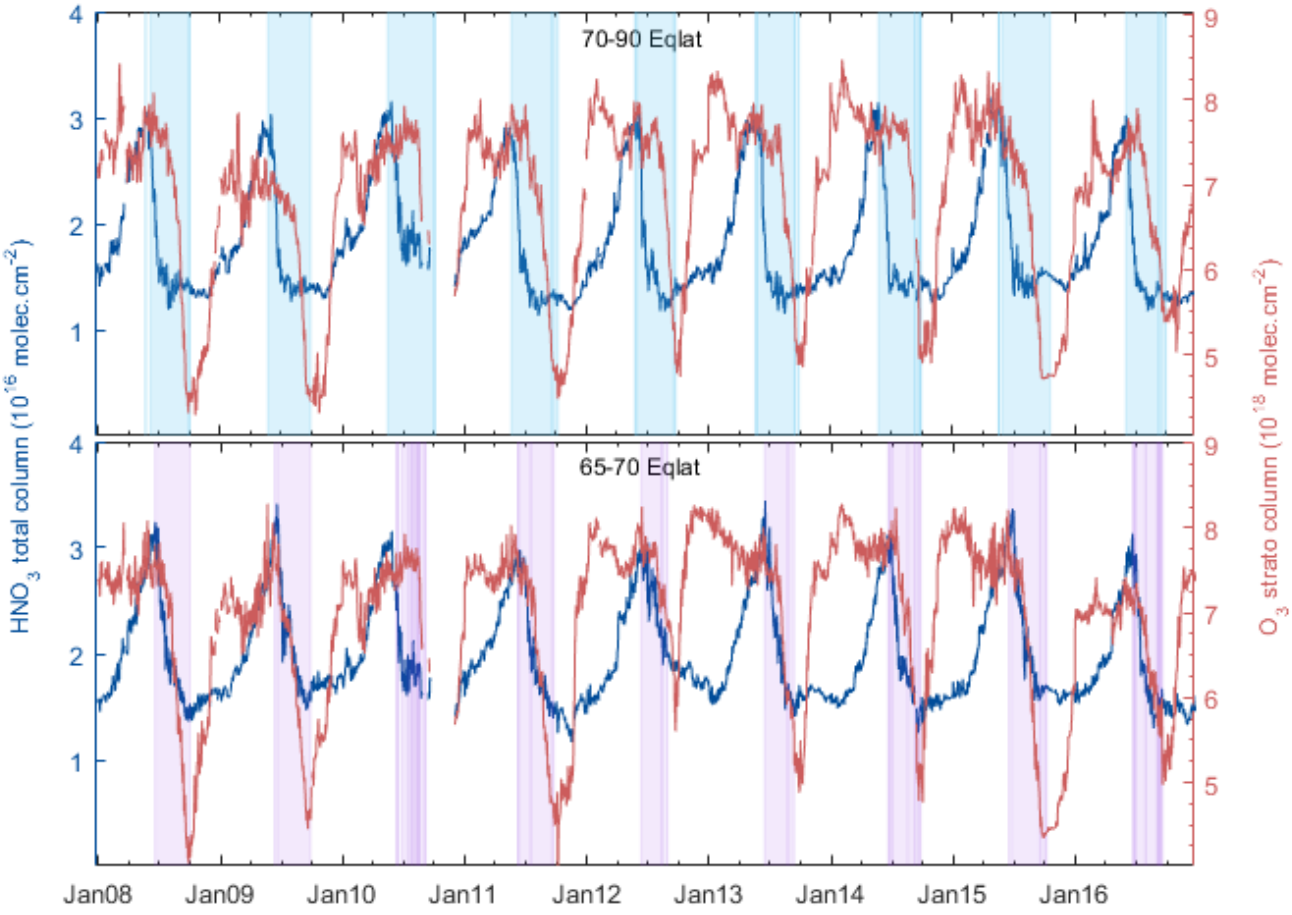

Figure 2. Total columns of HNO_3 (blue) and stratospheric columns of O_3 (red, both expressed in molec.cm^{-2}) for eqlat bands 70-90 S and 65-70 S. The vertical shaded areas in each panel are the periods during which the temperature was equal to or below 195 K in that band.

Further, I suspect that the very late recovery of HNO3 may have more to do with chemistry, in particular the fact that perpetual sunlight means NO3 is photolyzed effectively throughout the polar summer so that little of it can end up in N2O5 and hence to HNO3. This may do a better job explaining the ramp from Mar-May (e.g., in Fig 4) than other explanations, and could be probed fairly simply using chemical kinetic equations considering length of night, temperature, and ozone near 20-25 km. Zonal means should suffice, despite the potential for vortex meandering, which is likely to be small in summer.

Further discussion was added in the text in view of the Figure above and the very useful explanation of the referee in order to clarify the late recovery of HNO_3 columns after the winter. We now explain, also relying on literature, that up until the end of September (end of the winter), the low columns are attributable to the formation of PSCs with the low temperatures and further sedimentation of PSCs, which heavily denitrifies the stratosphere. The persistence of low columns in spring and summer is then rationalized by very effective photodissociation of HNO_3 and NO_3 during the periods of prolonged sunlight, i.e. late spring and summer. Also, local minima of temperatures that stay below 195 K could cause a slower recovery too. This section in the text now reads: *"… with previous studies by McDonald et al. (2000) and Santee et al. (2004) for earlier years. However, the recovery of the HNO_3 total columns is very slow compared to other species, namely O_3, for which concentrations return rapidly to usual values almost as soon as PSCs disappear. In fact, the HNO_3 columns stay low well after the September equinox and are only subject to a slow increase 2 months later (in early December). While more persistent local temperature minima staying below 195 K could explain part of this late recovery, we make the hypothesis that it is due mainly to a combination of two factors: (1) a significant sedimentation of PSCs towards the lower atmosphere during the winter, yielding only small amounts of it to release HNO_3 under warmer temperatures (Lowe and MacKenzie, 2008; Kirner et al., 2011; Khosrawi et al., 2016), and (2) the effective photolysis of HNO_3 and NO_3 in spring and summer under prolonged sunlight conditions, i.e. mainly at the highest latitudes, which respectively increase the HNO_3 sink and reduce the chemical source (because NO_3 cannot react with NO_2 to produce N_2O_5, Solomon, 1999; Jacob, 2000; McDonald et al., 2000). The increase observed in March, at the start of the winter, is in turn explainable by a much reduced number of hours of sunlight, implying less photodissociation. It is worth noting that the two regions previously mentioned (inner and outer vortex)…"* (p.5 line 23-35)

3) The authors often (not always, but often) refer to low HNO3 columns as synonymous with denitrification, but what about, for example, high ClONO2 columns associated with the collar implying that NOy may be in that form at times? Similarly, the low HNO3 during mid-summer seen in Figure 4 and discussed above may have to do in part with perpetual sunlight meaning high NO and NO2 amounts, with less in HNO3 but not necessarily less total NOy. Some further discussion is merited.

We thank the referee for pointing this out. We have taken care in the revised manuscript to not mix denitrification with loss of HNO_3, and replaced the abusive "denitrification" terms with "loss of HNO_3", "decreasing HNO_3 columns, "decrease in HNO_3", …

Response to Referee #2

First, we would like to thank Referee #2 for his/her careful and expert reading of the paper as well as for his/her questions and suggestions. We have taken all the comments into account and have tried to address each as thoroughly as possible. We believe that the paper has been substantially improved thanks to the review.
The reviewer's comments are addressed here below on a point-by-point basis, with the initial comment reproduced in blue first.

General comment:

1) One general – though minor and easily rectified – comment is a pervasive lack of adequate referencing throughout the manuscript. PSC formation and denitrification, and their roles in chlorine activation and chemical ozone loss, are extremely well-studied phenomena, and obviously it is not possible (or even desirable) to cite every paper on these topics published in the last 30 years. But in many places the authors have chosen to cite only a few papers for well-known points, without prefacing the list with "e.g.". This may seem like a petty point, but not only does their selection of which papers to reference often come across as arbitrary, but also their approach may give non-expert readers the impression that only those few highlighted papers are of relevance. So I suggest going through the manuscript and adding "e.g." in front of the list of cited papers in many places. Some specific examples of where this is needed include: p2, L4; p2, L6; p2, L8; p2, L19; p2, L23; p8, L2; p8, L4; p8, L7; p8, L17; p8, L18; p8, L24.

The mention "e.g." was added everywhere as was suggested by the reviewer. A few additional references were also included to be more exhaustive, for example:

- p. 1 line 20
- p. 4 line 19
- p. 4 line 31
- p. 5 line 19
- p. 8 line 28
- p. 9 line 31
- p. 14 line 34
- p. 15 line 10

Similarly, although the source (typically a URL) for each proxy is given in Table 1, I feel that it would be appropriate to provide a general citation in each sub-section of Section 4.3 where a given proxy is introduced. For example, references to published literature are needed on p7, L27 for F10.7, p8, L14 for MEI, and p8, L21 for AO and AAO.

General references were added for the description of the proxies:

- For the solar flux: *"…,and correlates to the number of sunspots on the solar disk (Covington, 1948; Tapping and DeTracey, 1990; Tapping, 2013)."* (p. 8 line 24-25)
- For the MEI: *"…, surface air temperature and cloudiness fraction (Wolter and Timlin, 1993, 1998)."* (p. 9 line 14)
- For the AO/AAO: *"…in the northern and southern hemispheres, respectively (Gong and Wang, 1999; Kodera and Kuroda, 2000; Thompson and Wallace, 2000)."* (p.9 line 20-21)

Specific substantive comments and questions:

2) p2, L26: I do not think it is true that "most often" MLR studies use an iterative selection procedure to identify relevant explanatory variables. In fact, I believe that only a handful of the many MLR ozone studies have done so. (And it seems strange to say "most often" and then cite only one reference.)

We agree with this remark. We have removed the "most often" and changed the sentence to "*In various multivariate regression studies, an iterative selection procedure is used to isolate the relevant variables for the concerned species*" (p. 2 line 26-27). Regarding the reference, it was initially meant to lead the reader to a paper describing that method (Mäder et al., 2007). However, for more completeness, other references have also been added: (Steinbrecht, 2004; Mäder et al., 2007; Knibbe et al., 2014; Wespes et al., 2016, 2017). (p. 2 line 26-28)

3) p3, L30: Does the cloud screening of IASI data include PSCs?

The cloudiness in the IASI pixel is estimated from the Advanced Very-High-Resolution Radiometer (AVHRR) satellite imager. The AVHRR observations are mapped inside the IASI pixel to determine the mean percentage of cloud cover in each IASI pixel. A maximum threshold of 25% for the cloud cover has been chosen for considering the IASI pixel as clear for the HNO_3 retrievals. While thick cirrus clouds have detectable signatures in the IASI spectra (on the longwave part of the spectrum), we have not been able to see any feature in the presence of PSCs, which are presumably absorbing IR radiation much too weakly. With this in mind, it is safe to say that scenes with PSCs are not flagged as cloudy and will not be filtered out by the operational processing for the HNO_3 retrievals.

Note also that the PSCs have, to the best of our knowledge, never been detected from the nadir spectra. They have already been measured from infrared limb sounders such as MLS, MIPAS (e.g. Höpfner et al. 2006, 2009; Nakajima et al., 2016) which have a longer observing path.

4) p4, L9: The PSC formation threshold is stated to be 195 K. It is fine for the purposes of this kind of analysis to use a constant value to indicate the likely presence of PSCs, but it should be acknowledged that the temperature at which NAT forms varies with altitude and time over the season, and thus this value is approximate.

We thank the referee for making this point, on which we fully agree. The figure below gives HNO_3-temperature correlations for the stratosphere and it is indeed seen that low HNO_3 columns occur also at lower or higher temperatures than 195 K (namely between 190 and 200 K), on a local scale. This section was adapted to clarify this and put more caution on the 195 K threshold: *"… (195 K, based on ECMWF temperatures). It should be noted that while this temperature is a now widely accepted approximation for the formation threshold for NAT (type I), its actual value can be different depending on the local conditions (Lowe and MacKenzie, 2008; Drdla and Müller, 2010; Hoyle et al., 2013). Also, other forms of PSCs, particularly the type II PSCs (ice clouds) form at a lower temperature of 188 K, corresponding to the frostpoint of water, or 2-3 K below that (e.g. Toon et al. (1989); Peter (1997); Tabazadeh et al. (1997); Finlayson-Pitts and Pitts (2000))."* (p. 4 line 16-20)

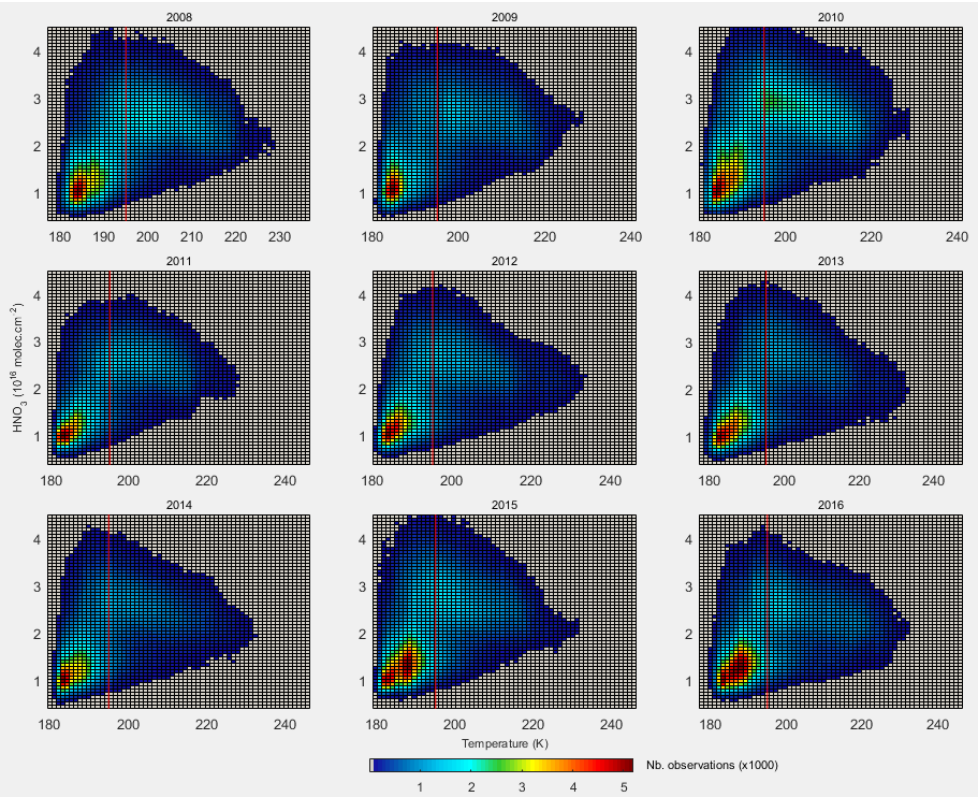

Figure 1. Total columns of HNO_3 (10^{16} molec.cm^{-2}) VS temperatures (K) for the 70-90 S eqlat band and between May and October. The color scale indicates the number of measurements per bin (with grey areas for bins with less than 80 measurements), and the red line is the 195 K threshold.

5) p5, L4-5: It is true that these IASI results confirm earlier findings, and references are needed here.

We had references for this further in the text, but we agree that they are needed here too. The references (McDonald et al., 2000; Santee et al., 2004; Lambert et al., 2016) have been added. (p. 5 line 15)

6) p5, L9-11: I find this part of the discussion confusing. First, it is stated that the "delayed denitrification" in the 65-70S band is attributable to "the later appearance of PSCs" and "the mixing of these air masses with the denitrified air masses from the center of the vortex". Are the authors asserting that some of the decrease in HNO3 observed in the 65-70S band does not arise directly from PSC sedimentation within that band, but rather from dilution of HNO3 abundances through mixing with denitrified air masses from deeper in the vortex core? In that case, the decrease in HNO3 should not be called "denitrification". More importantly, is this suggestion consistent with the findings of Roscoe et al. [JGR 117, 2012] that the broad vortex edge region is only weakly mixed with the deep core during the winter?

We would like to thank the referee for this comment and the reference mentioned. Indeed, we had initially attributed the delay in denitrification to the mixing of air masses between the two regions of the vortex in addition to the PSC sedimentation (the purple shaded areas in Fig.2 indicate the threshold temperature for the PSC Ia formation). It is however clear, following the above reference and others, that this process is unlikely to contribute significantly. The text was accordingly changed to: "*The delayed decrease in HNO_3 in the outer parts of the vortex (i.e. in the 65-70 S eqlat band) can thus be attributed to the later appearance of PSCs in this region (see Figure 2 purple shaded areas in second panel).*" (p. 5 line 17-18)

Also, mention of the separation between the two parts of the vortex is made further in the text: "*It is worth noting that the two regions previously mentioned (inner and outer vortex) have been observed to behave differently; the inner vortex (70-90 S) undergoes strong internal mixing whereas the outer vortex (65-70 S), isolated from the vortex core, experiences little mixing of air. This, combined to a cooling of the stratosphere, could lead to increased PSC formation and further ozone depletion (Lee et al., 2001; Roscoe et al., 2012).*" (p. 5 line 35 – p. 6 line 3)

Second, the next sentence states that these "two processes lead to the total columns in both eqlat bands being in the same range of values by the end of December". The Antarctic vortex is breaking down (or has mostly broken down) by the end of December, so of course mixing at this time homogenizes the high-latitude HNO3 distribution, but it doesn't make sense to be talking about the later appearance of PSCs in this context.

Following the changes made with regard to the previous point, this sentence was also modified to: "*By the end of December, i.e. when the vortex has started breaking down (e.g. Schoeberl and Hartmann, 1991; Manney et al.,1999; Mohanakumar, 2008), the total columns in both eqlat bands homogenize and reach the same range of values ($1.7x10^{16}$molec.cm^{-2}).*" (p. 5 line 19-21)

7) p5, L16-18: I also find these sentences confusing. It is stated that the columns in the 55-65S band keep increasing during the low-temperature periods, but cold intervals are not marked for that eqlat band. Are the authors referring to periods that are cold at higher latitudes? If so, then this statement is not entirely correct, as HNO3 values at 55-65S start to decline from their peak values while temperatures are still low in the 70-90S and 65-70S bands. The maximum in HNO3 values in June-July is attributed to "less sunlight compared to lower latitudes", but the comparison shouldn't be to lower latitudes but rather midwinter vs summer (at the same latitude).

With this sentence, we meant that the HNO_3 columns in that eqlat band do not drop as suddenly as at higher latitudes, with regard to the start of the low temperatures at higher

latitudes. We agree that the formulation was not sufficiently clear and the sentence was therefore changed to: "*…, we show that the columns in that band keep increasing when the temperatures at higher latitudes start decreasing, to reach maximum values of about 3.4x10^{16} molec.cm^{-2} in June-July; this is due to a change in the NO_y partitioning towards HNO_3, itself due to less sunlight compared to the summer."* (p. 6 line 6-8)

> In addition, the role of confined diabatic descent inside the vortex should be mentioned, as it is a major factor leading to strongly enhanced wintertime HNO3 abundances in the lower stratospheric layer to which the IASI column amounts are most sensitive.

The role of this diabatic descent was mentioned in the part analysing the annual cycle in Section 4.4.3 (p. 13 line 25-29). However, we agree with the referee that it would be good to include it here first, since we indeed already describe the higher columns recorded during the winter. This section thus now reads: "*Also inducing increased concentrations during the winter at high latitudes is the diabatic descent occurring inside the vortex when the temperatures decrease. This downward motion of air enriches the lower stratosphere in HNO_3 coming from higher altitude (Manney et al., 1994; Santee et al., 1999), yielding higher column values which are, in this eqlat band, not affected by denitrification."* (p. 6 line 9-12)

8) p5, L23-24: The statement that temperatures in the northern high latitudes rarely reach the PSC formation threshold is much too general. While that is true for the polar-cap (70-90N) average being considered here, temperatures in the Arctic lower stratosphere certainly do drop below PSC formation thresholds in localized regions in almost every year. Moreover, it is not the *average* temperature – which is what I believe is being shown in Figure 2, although it's not clear – that is important for PSC formation. It is the *minimum* temperature that is important. In fact, if indeed Figure 2 is showing eqlat band average temperature, then it should be reformulated to correlate HNO3 behavior with the minimum temperatures in that band. In any case, the exact nature of the temperatures being shown should be specified (at the beginning of Section 3 and in the caption).

We agree with this general statement that temperatures in the northern hemisphere can locally reach below 195 K. However, we feel that for the purpose of the paper and the analysis, we should stick to average temperatures (what is shown here). Indeed, it makes more sense to us to talk about average temperatures when we treat average HNO_3 total columns. However, for the sake of completeness, we show the minimum temperatures in the Figure below. While local minima are indeed observed in the minimum temperatures (last panel), the general pattern of temperatures below 195 K is the same as when considering the average temperatures (5th panel). For this reason, and because we had rather stay consistent with the average HNO_3 total columns, we decided to keep the average temperatures. The legend of Figure 2 in the paper was completed: "***Figure 2**. (four top panels) HNO_3 total columns time series for the years 2008-2016, for equivalent latitude bands 70-90, 65-70, 55-65 and 40-55, north (green) and south (blue). Vertical shaded areas are the periods during which the average temperatures are below T_{NAT} in the north (green) and south (blue) 70-90° band, and in the south (purple) 65-70° band. Note that the large period without data in 2010 is when there was a low amount of data distributed by EUMETSAT (see Section 2). (bottom panel) Daily average temperatures time series (in K) taken at the altitude of 50 hPa for the equivalent latitude bands 70-90° North (green) and South (blue) and 65-70° South (purple). The horizontal black line represents T_{NAT} , i.e. the 195 K line."* (p. 29)

Note also that mention of this was added in the text: *"The northern hemisphere high latitudes usually do not experience denitrification, mostly because the temperatures, while sometimes showing local minima below 195 K, rarely reach the PSC formation threshold on broad areas and for long time spans (see Figure 2 for average temperatures, light green vertical areas). A few years stand out, however, …"* (p. 6 line 16-18)

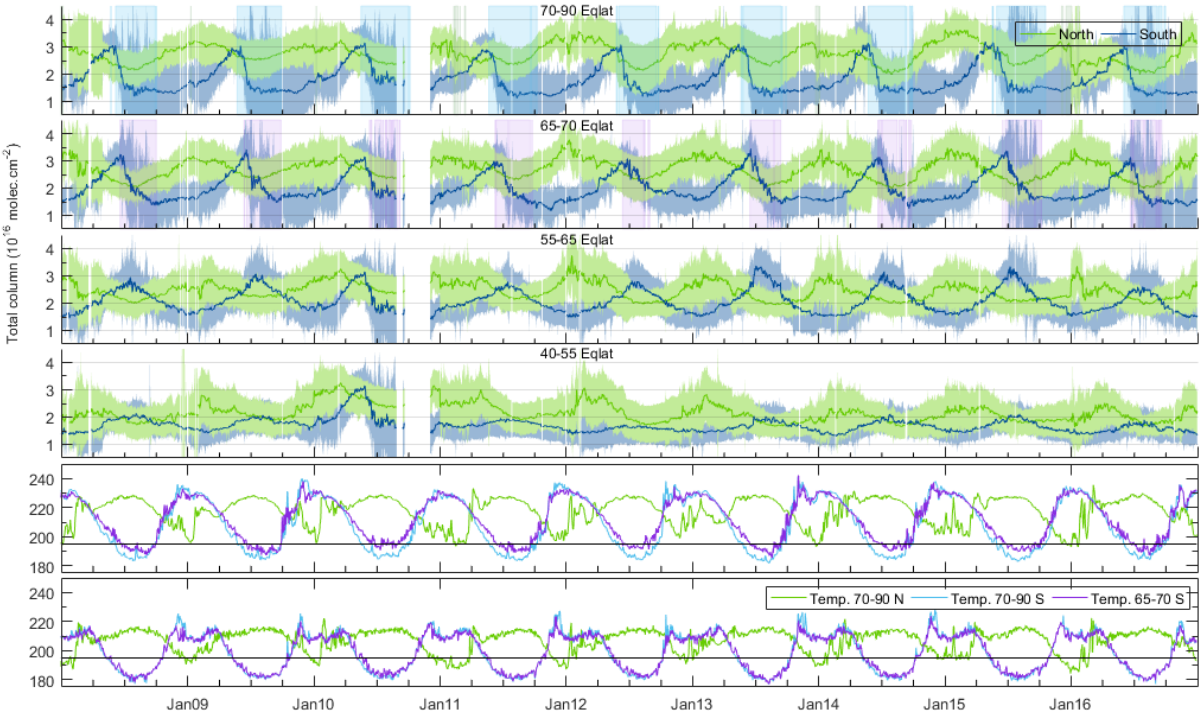

Figure 2. As Figure 2 in the text (see reproduced legend between quotes above). The 6th panel is the minimum temperatures time series (in K) for eqlat bands 70-90 N (green), 70-90 S (blue) and 65-70 S (purple).

9) p6, L4-5: For ease of reference, the lack of IASI data in September-December 2010 should be first noted in Section 2, where the data set is described. It seems to me that this interval is also noticeable in Figure 2, so I suggest removing the data during this period in that Figure as well.

We thank the referee for this remark. The explanation for this lack of data is now mentioned in Section 2, when describing the IASI data. The sentence was transferred from one section to the other, and is now: "*…, i.e. all scenes with a higher fractional cloud cover than 25% are not taken into account. It should be noted that there was an abnormally small amount of IASI L2 data distributed by EUMETSAT between the 14th of September and the 2nd of December 2010 (Van Damme et al., 2017), and that these data have been removed from the figures and analyses in the following of the paper. For the present study,…"* (p. 3 line 32 – p.4 line 3)

The part in Section 3 reads in turn: "*… in the northern (top) and the southern (bottom) hemispheres. July and August of 2010 stand out in the Antarctic, with high and variable columns…"* (p. 6 line 32-33)

Figure 2 was updated by removing these data. (p. 28)

10) p6, 7-9: It is hypothesized that the anomalous behavior in July-August 2010 seen in IASI HNO3 data was a consequence of descent induced by the midwinter minor warming. It seems to me that a more obvious explanation is that the SSW caused lower stratospheric temperatures to rise sufficiently that PSC formation was temporarily inhibited. It is worth noting in the manuscript that a similar evolution of HNO3 was recorded by Aura MLS in that winter, as shown in Figure 3-6 of the 2014 WMO Ozone Assessment. The 2014 WMO Report also showed that in 2010 VPSC (based on MERRA) remained well below the 1979-2012 Antarctic average and less denitrification than typical occurred.

Indeed, we conducted further research on the topic, thanks to the reference mentioned in this comment, and adapted this section accordingly: "*…, with high and variable columns*

recorded by IASI. This is a consequence of a mid-winter (mid-July) minor sudden stratospheric warming (SSW) event that induced a downward motion of air masses and modified the chemical composition of the atmosphere between 10 and 50 hPa and until at least September (de Laat and van Weele, 2011). This is a consequence of a mid-winter (mid-July) minor sudden stratospheric warming (SSW) event that induced a downward motion of air masses and modified the chemical composition of the atmosphere between 10 and 50 hPa and until at least September (de Laat and van Weele, 2011; Klekociuk et al., 2011). The principal effect of this sudden stratospheric warming was to reduce the formation of PSCs (which stayed well below the 1979-2012 average, WMO (2014)) and hence reduce denitrification. This is shown by an initial drop in June, as is usually observed in other years but then by an increase in HNO_3 columns when the SSW occurs. These results confirm those previously obtained by the Aura MLS during that winter and reported in the World Meteorological Organization (WMO) Ozone Assessment of 2014 (see Figure 6-3, WMO (2014)). Apart from these peculiarities for the year 2010,…" (p. 6 line 33 – p. 7 line 5)

11) p10, L20-21: I find this discussion confusing. First, a *delay* in the drop in HNO3 concentration in the fit for the 65-70S band is noted, but then it is stated that it "happens *earlier* than in the IASI observations since the VPSC proxy is based on temperatures and composition *north* of 70". Figure 6 does show that the fitted midwinter peak in HNO3 slightly precedes that observed, so I assume that "earlier" is correct and "delay" must be a typo. However, it is also true that the HNO3 decline is more gradual in the model than in the data, so that in late winter the fit line lags the observations. Exactly which behavior is being discussed should be clarified. Also, since it is the Antarctic that is being talked about here, "north" should be "poleward".

We apologize for the confusion in this paragraph. What is meant here is that, in the 65-70 S eqlat band, the fit calculated by the model is lagged in time (happens slightly earlier) compared to the observations in that band, because the VPSC proxy is based on the temperatures of the 70-90 S eqlat band, where the drop happens earlier. Hence the fit in the 65-70 S band simulates a drop earlier than is actually observed in that band. We hope this makes the understanding of this section easier, and decided, as suggested, to clarify it in the manuscript to avoid any future confusion. This section is now: "*This translates to a lag between the observations in the 65-70 S eqlat band and the fit in which the drop of HNO_3 concentrations happens earlier than in the IASI observations. This is explained by the fact that the VPSC proxy is based on temperatures and composition poleward of 70°. It induces a lower correlation coefficient (0.87) and…".* (p. 11 line 21-23)

12) p10, L27-28: The deep minima in HNO3 in the northern polar regions in October 2014 and 2016 almost certainly have nothing to do with denitrification during the preceding Arctic winters. Any signature of denitrification gets completely obliterated when the vortex breaks down at the end of winter. Even in the Antarctic, where denitrification is severe every winter, its signature is not still visible in the high-latitude HNO3 abundances the following fall. The extremely low 70-90N HNO3 values in October 2014 and 2016 (and also 2012, when the residuals are particularly large) are indeed quite interesting, but they cannot be ascribed to denitrification. It's possible that the low HNO3 observed in boreal fall 2016 may have been linked to the QBO disruption [e.g., Tweedy et al., 2017].

We thank the referee for this remark. It was not our intention to imply a causality link between the exceptional Arctic denitrification events and the unusual lows recorded in the HNO_3 columns. To clarify this, we changed the formulation to: "*In the same way, a few pronounced lows recorded by IASI, especially those in the Northern polar regions (mid-June to early October 2014 and 2016, for instance) are not captured by the model."* (p. 11 line 28-30)

As for the QBO disruption: we agree that it could have an effect on the HNO_3 behaviour in polar regions, but it is not suggested by the model, where the inclusion of the QBO proxy does not improve the model/observations misfit in 2016. To asses this further and because

this disruption occurred around 40 hPa (e.g. Newman et al., 2016, Tweedy et al., 2017), we tested the inclusion of the QBO at 50 and 20 hPa (rather than a 30 and 10 hPa). This yields similar results (see Figure below) for all years – including 2016 – and therefore suggests that QBO is not the driving effect for the deep minima.

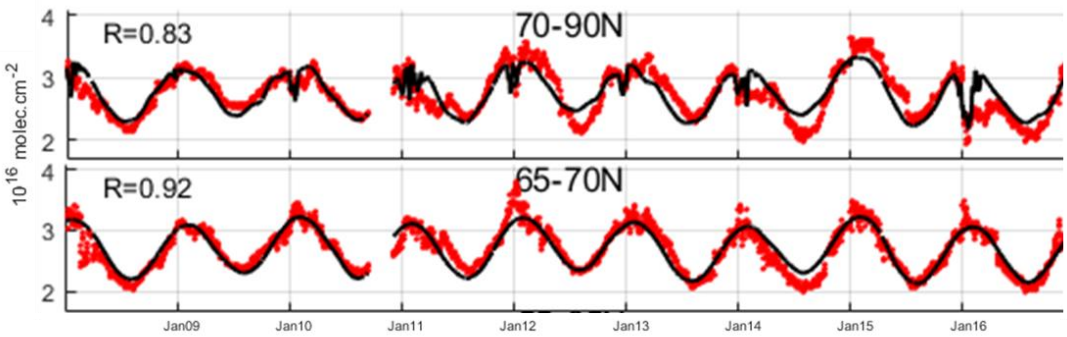

Figure 3. IASI HNO_3 total columns (red dots) for the 2 northernmost eqlat bands and the associated fitted model (black curves) featuring the QBO at 20 and 50 hPa.

13) p11, L14-15: It is noted that parts of Eurasia stand out with a low percentage of observed variability explained by the model. Could this be related to the low sensitivity of IASI data in this region, where the elevated terrain of the Tibetan Plateau reduces the signal-to-noise of the retrieval (e.g., Luo et al., ACPD 2017)?

We believe there might be some confusion here, as to what area was meant: the low percentage of explained variability that we are mentioning here refers to the area above Kazakhstan and the west Siberian plains, which are rather low in altitude (compared to the Tibetan Plateau, anyway). We have added this in the text to clarify the point: *"…although some continental areas (Northern part of inner Eurasia above Kazakhstan and the west Siberian plains) stand out with percentages..."* (p. 12 line 16-17)

Regarding the low sensitivity of IASI that the reviewer is referring to, it is a feature specific to tropospheric species such as CO.

Regarding HNO_3 columns, since the sensitivity of IASI is mostly in the stratosphere, the retrievals are barely affected by topography. Furthermore, retrievals with weak signal-to-noise ratio and small degree of freedom for signal would translate to a weak detected variability in IASI HNO_3, but not to a weak explained variability by the regression model.

14) p11, L16-21: The low fraction of explained HNO3 variability in the tropics and subtropics is attributed to lightning NOx production. In addition to sources, unaccounted-for sinks of HNO3 should also be considered, such as scavenging in convective updrafts and cirrus clouds.

We thank the referee for this remark. Indeed, some HNO_3 sinks are most probably also unaccounted for, and mention of this was added in the text: *"... missing some of the variability recorded in the observational data. Another cause for the discrepancies between the observations and the model could be unaccounted sinks of HNO_3, such as deposition in the liquid or solid phase and scavenging by rain. It should be noted that a small area of high explained variability is observed in Africa, …"* (p. 12 line 24-27)

15) p11, L27-28: If the signal over southern Africa induced by NO2 from biomass burning is being carried by the annual term in the model, then shouldn't the coefficients a1 or b1 be larger in that region in Figure 11 (which is not the case)?

Indeed, it should, and it actually is, but to a lower extent than the signal elsewhere on the globe. Because of the color scale chosen for the a_1 and b_1 distributions, it does not appear clearly. The color scale was chosen to avoid complete saturation in the northern latitudes. Here the same figure is reproduced with a different color scale, where the largest (negative) influence of the a_1 coefficient appears more frankly in southern Africa (see top left panel):

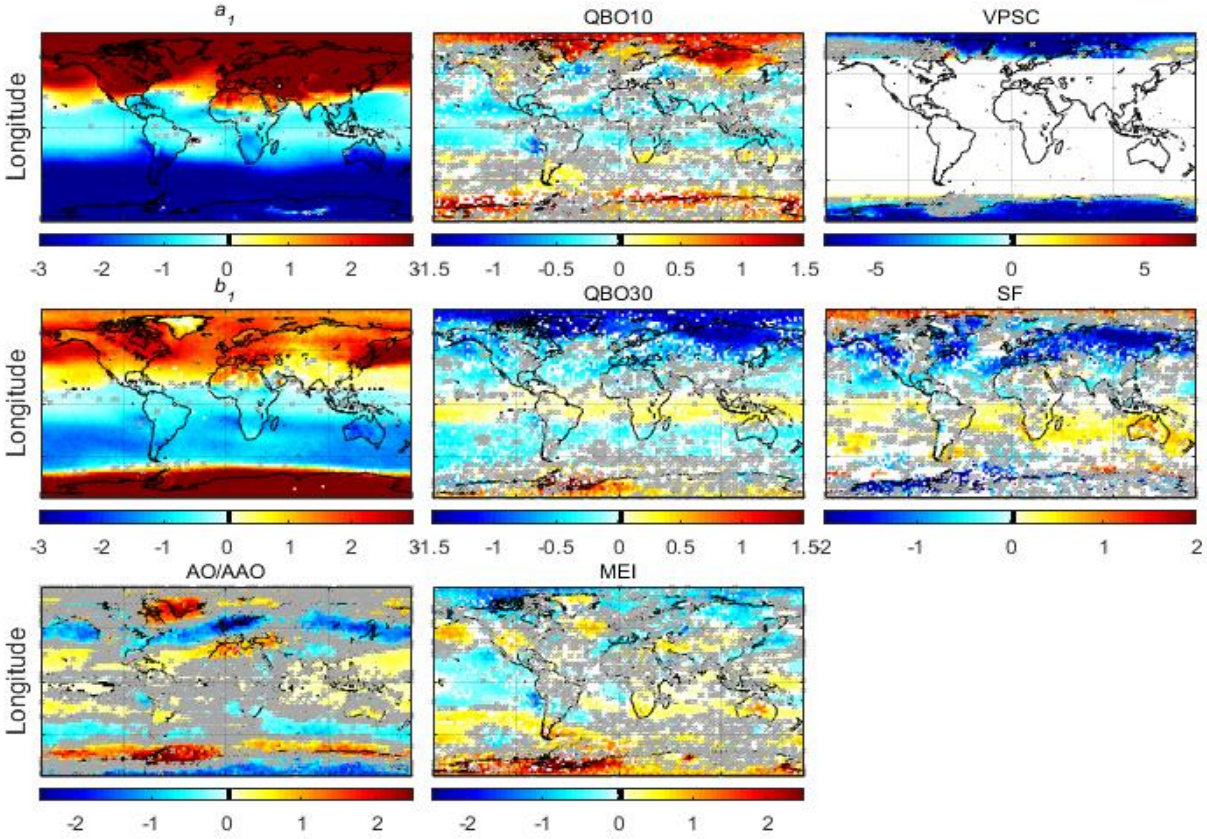

Figure 4. Global distributions (2.5° x 2.5° grid) of the regression coefficients expressed in 10^{15} molec. cm^{-2}. The contrast of a_1 and b_1 were modified in order to enhance the negative signal above south Africa.

We added mention of this in the text: "*Indeed, the large vegetation fires of Africa every year around July emit the largest amounts of NO_x (compared to large fires of South America, Australia and southeast Asia). Their influence translates to an overrepresentation of the annual term (up to -2x10^{15} molec.cm^{-2}) in the fitted model (although not clearly visible in Figure 11 because of the color scale chosen). This larger contribution of the annual variability thus yields…".* (p. 12 line 30-33)

16) p12, L1-2: It might be good to mention the issues with the retrievals caused by elevated terrain here as well.

See also answer to comment 13: The topography does not cause any particular problem for the retrieval of HNO_3. The degree of freedom for signal and retrieval total errors are only slightly smaller and larger, respectively, above elevated surface. This is more the case in the tropical regions where the tropospheric HNO_3 represents a large part of the total HNO_3 (e.g. Ronsmans et al., 2016).

17) p12-13, Section 4.4.3: I appreciate that the authors limited the number of figures, showing only the regression coefficient for each proxy (Figure 11) and not the fraction of HNO3 variability it explains. But the accompanying discussion frequently refers to the percentage contribution from specific proxies. Although some sense of their relative importance in different regions can be obtained from Figure 11 (and also Figure 8), I suggest either adding "(not shown)" everywhere a percentage contribution is discussed in this section or adding (and referring to) another figure containing this information.

Indeed, while we asked ourselves the question of a supplementary figure a few times, we decided not to add it in order to focus the reader on the essential figures. The percentages we use in the discussion of the distributions of the coefficients are obtained from the formula described in the 'introductory' part of that section ($[\sigma(X_i)/\sigma(HNO_3^{IASI})\times 100]$). We do agree that the source of those percentages may be forgotten as one reads on through the manuscript. In order to keep the text as understandable as possible, we have chosen to add a sentence in the introductory part to insist on the use of the equation: *"…, and expressed in %. Note that, although the distributions of the contribution of each proxy are not shown as a Figure, the calculated percentage values are used in the following discussion (next 3 sections) to quantify the influence of the fitted parameters."* (p. 13 line 11-13)

18) p12-13, Section 4.4.3: I would have liked to have seen a bit more discussion of whether these results for HNO3 are consistent with previous MLR analyses of ozone data that included similar terms. In particular, the SF results are not put into the context of previous findings.

The paragraph was adapted in order to put our results in parallel with previous similar studies that addressed the question of the influence of the solar cycle on ozone. It was found that the behaviour of HNO_3 is mostly different from that of O_3 in most studies, in that we obtain a negative signal in the northern hemisphere. Mention of this is provided in the text as follows: *"… or negative elsewhere. Previous studies showed that ozone changes due to the solar cycle are largest in the low stratosphere (Hood, 1997; Soukharev and Hood, 2006), which corresponds to the altitude of maximum sensitivity for HNO_3. Our results for the mid to high latitudes suggest opposite behaviour for HNO_3 (as was also reported for O_3 by Wespes et al. (2017)). However, the positive contribution of the solar cycle on the HNO_3 variation in the tropical stratosphere is in line with the low-latitude O_3 response previously reported (Soukharev and Hood, 2006; McCormack et al., 2007; Frossard et al., 2013; Maycock et al., 2016)."* (p14 line 5-10)

In addition, the positive signal above the southern polar region is characterized as "weak", but in fact the largest positive MEI regression coefficients are found over Antarctica. Is that in line with expectation?

First, we would like to notify the reviewer that we did as for the solar cycle; we added references of previous studies in the text: *"…, and in the mid-latitudes of the northern hemisphere. The east-west gradient is in good agreement with chemical and dynamical effects of El Niño on O_3, and with previous studies that showed the same patterns for the influence of the MEI on O_3 (Hood et al., 2010; Rieder et al., 2013, Wespes et al., 2017)."* (p. 14 line 17-19)

As for the strong positive signal over west Antarctica, general caution should be taken when it comes to the results in that particular area of the southern polar regions. This region often shows unexpected retrieved concentration profiles for HNO_3 (see also the RMSE distribution in Figure 9, bottom), that we interpret as erroneous. This is likely related to emissivity issues in that region (mentioned in Section 4.4.2, p. 13 line 2-6) and in particular the fact that ice-shelf is treated with a constant ocean-like emissivity.

To avoid misinterpretation of this, we have added the following when describing the distribution of the coefficients: *"Note also that the strong negative signal observed above western Antarctica is most probably due to the drawback of using for all seasons a constant*

emissivity for ocean surfaces (e.g. even when the ocean becomes frozen). For this reason, the regression coefficients in this area will not be discussed further." (p. 14 line 10-13)

> Previous studies looking at the influence of AO/AAO on ozone are alluded to on p13, L8, but no references are given there, and it is not clear whether the citations in the next sentence are relevant for this point (e.g., the 2009 paper by Wespes et al. is about HNO3 and does not discuss the AO/AAO).

All references were listed at the end of this paragraph, but we agree that it is confusing. In the revised manuscript, we have divided the references between those for similar MLR studies and those detailing the influence of the AO/AAO in the atmosphere in general. Also, the reference of Wespes et al. 2009 was a typo, we meant Wespes et al. 2017. We thank the referee for his careful reading and apologize for this. The paragraph now reads: *"These results are in agreement with previous studies that showed that, for O_3, both the arctic and antarctic oscillations (also called "annular modes") are leading modes of variation in the extratropical atmosphere (Weiss et al., 2001; Frossard et al., 2013; de Laat et al., 2015; Wespes et al., 2017).They largely influence the circulation up to the lower stratosphere and represent, particularly in the southern hemisphere, the fluctuations in the strength of the polar vortex (Thompson and Wallace, 2000; Jones and Widmann, 2004; van den Broeke and van Lipzig, 2004). This further shows the similarity in the behaviour of O_3 and HNO_3."* (p. 14 line 24-29)

> The influence of the QBO in the equatorial regions is noted, but no mention is made of the fact that the coefficients are much larger at northern high latitudes.

Indeed, this point needed further explanation. This section in the text was completed in order to describe the potential influence of the QBO in the extratropics: *"Even though the QBO is a tropical phenomenon, its effects extend as far as the polar latitudes, through the modulation of the planetary Rossby waves (Holton and Tan, 1980; Baldwin et al., 2001). Because there are more topographical features in the northern hemisphere than in the southern hemisphere, these waves have a larger amplitude and can influence the polar stratospheric temperatures and hence the vortex formation. While the exact mechanism for the extratropical influence of the QBO is not exactly understood (Garfinkel et al., 2012; Solomon et al., 2014), it seems the large positive and negative signals observed in the northern high latitudes in Figure 11 can indeed be attributed to this modulation of the Rossby waves by the oscillation in the meridional circulation. This was also observed for O_3 by e.g. Wespes et al., (2017)."* (p. 14 line 33 – p. 15 line 5)

19) p14, L32-33: I do not wish to take away from the value of the IASI HNO3 measurements, whose dense spatial coverage and long-term record are obviously of great benefit, as this study has shown. But I would ask for a bit more care in the language used here. Although the novel statistical nature of these results is mentioned, I think that some readers could take away from these lines the message that this analysis has revealed the profound influence of PSC formation and denitrification on the HNO3 distribution, when in fact the crucial role of those processes has been known for decades. In truth, it is not obvious to me what additional knowledge about the variability of HNO3 in the polar regions has been gained from this study that had not been demonstrated previously using limb measurements with much coarser horizontal but much greater vertical resolution.

We agree with the reviewer that the results presented in this study have been exposed in previous studies. This work allows confirming well-known processes thanks to the use of a multivariate regression model applied for the first time on HNO_3 time series. This sentence was modified: *"The amount of data allows for a thorough monitoring of the processes regulating the HNO_3 variability, such as the denitrification processes in the southern polar regions, as well as the seasonal variability in the tropical regions."* (p.16 line 21-23)

20) p25, Figure 2: Minor tick marks on the y-axis would be helpful.

Minor ticks on the y-axis have been added on all subplots.

As mentioned earlier, it might be good to remove the sparse measurements during the September-December 2010 interval from this plot as well.

Thank you for this remark. The data for the period in 2010 where too few measurements are available have been removed and the legend of the figure was adapted accordingly.

Why do some of the vertical lines, especially (but not only) in the purple 65-70 eqlat region, appear to be thicker? Is it because temperatures are hovering around the PSC threshold at those times, so the shading is being turned off and on multiple times in quick succession?

Yes indeed, the reason for the impression of thicker lines is due to the fact that the temperatures are oscillating around the 195K threshold. However, the edges of each 'patch' was also darker, in order to identify more clearly the start and end of each period under 195K. After several visual tests, it was decided to remove this darker edge, as it did not seem necessary. This allows limiting the impression of ticker lines (particularly visible in the 65-70 S eqlat band during denitrification). (p. 28)

21) p30, Figure 7: Why is there a break in the without-VPSC fit curve in the 70-90S panel in October-November 2014? Such a break does not appear in the similar panel for the with-VPSC fit (or in Figure 6).

We would like to thank the reviewer for that remark. It is actually an error in the plotting that escaped our attention. There is actually no missing data and this was rectified. Note also that there was an error in the figure initially submitted. The time series of IASI, the fit and the residuals (two top rows) were not correctly aligned with the time series of the PSCs. This was also corrected in the revised version of the paper.

22) p33, Figure 10 caption: The wording of the caption ("Time evolution of IASI HNO3 (red) and NO2 (green)") implies that the NO2 data are from IASI, but the reference cited is for GOME-2 data. Please clarify.

Indeed, this is a mistake. The NO_2 data come from GOME-2, and not from IASI. The caption was rectified and now reads: "*Time evolution of IASI HNO_3 (red) and GOME-2 NO_2 (green) from 2008 to 2015 for Africa…"* (p. 36)

Minor points of clarification, wording / figure suggestions, and grammar / typo corrections:

23) p1, L13: "PSCs" should be defined in the abstract as well as the main body of the paper.

The full name is now used in the abstract, followed by the acronym between parentheses (p.1 line 13-14). The same is done in the text for the first mention (p.1 line 20).

24) p1, L23: inexsitent –> non-existent

The change was made (p. 1 line 23).

25) p2, L3: "PSCs" was already defined on p1, L20

The full name was replaced by the acronym only (p.2 line 3).

26) p2, L8: and further –> followed by

The formulation was modified (p. 2 line 8).

27) p2, L11, L14: These acronyms (UARS, MIPAS, ACE-FTS) should probably be spelled out. Also, "AURA" –> "Aura" and "ODIN" –> "Odin" (they are not acronyms, just names)

In order not to have too long sentences and/parentheses, it was decided to spell out the names of the instruments only, and to include them in a footnote. The acronym is kept in the text (p. 2 line 10-16 + footnote).

28) p3, L10: bi-daily –> twice daily ("bi-daily" could be interpreted to mean every two days)

The sentence was changed to: "*… consists of measurements taken twice a day (at 9.30 AM and PM, …)"* (p. 3 line 13-14)

29) p3, L15: The university name should be spelled out here

The full name is now included, followed by its acronym (p. 3 line 18-19).

30) p3, L24: Can 15-20 km really be considered the "low-middle" stratosphere? This seems more like just the lower stratosphere to me.

This was changed to "lower stratosphere" (p.3 line 27).

31) p3, L30: higher fractional cloud cover than 25% –> fractional cloud cover higher than 25%

This was modified (p. 3 line 33).

32) p4, L19: Further than –> Beyond

The modification was made (p. 4 line 28).

33) p4, L22: delete "columns" (some of the previous studies were based on HNO3 profiles, not columns)

The word "columns" was removed (p. 4 line 31).

34) p5, L14: delete "itself"

The word "itself" was removed (p. 6 line 4).

35) p5, L20: more –> longer

The word "more" was modified to "longer" (p. 6 line 13).

36) p5, L26: It would be good to add "Arctic" in front of "winters" and "over a broader area" after "threshold"

These two sentences were adapted: *"… and, to some extent, 2014 Arctic winters. During these three winters, temperatures reached below the 195 K threshold over a broader area and stayed low during a longer period than usual."* (p. 6 line 19-21)

37) p5, L35: "polar" –> "potential"

This word was changed (p. 6 line 30).

38) p6, L1: it's not clear why only one contour is noted here, when 3 contours of PV are shown in both hemispheres

The reference to the iso-contour was meant only for the last of the cited remarkable features. In order to make this clearer, the sentence was rephrased: *"…, the marked annual cycle at mid to high latitudes and the systematic and the occasional (2011, 2014, 2016) denitrification periods in the high latitudes of the Southern and Northern hemispheres respectively, which are highlighted by the iso-contours of potential vorticity at ±10x10^{-6} K.m^{2}.kg^{-1}.s^{-1} (dark blue)."* (p. 6 line 27-30)

39) p6, L4: EUMETSAT should be in all capital letters (as on p3, L29)

The word was capitalized (p.4 line 1).

40) p6, L12: dentrification –> denitrification

The word was corrected (p. 7 line 9).

41) p6, L14: What does "more stable" mean in this context? More constant over the season, or more uniform from year to year?? And what is the comparison against - wintertime values in the NH, or summertime values in the SH?

We apologize for the confusion here. The sentence has been rephrased: *"The northern hemisphere high latitudes (top panel) show more interannual variability than in the south, especially during the winter because of the unusual denitrification periods observed in 2011 (purple), 2014 (blue) and 2016 (black) in January (concentrations as low as 2.2x10^{16} molec.cm^{-2} in 2016). Contrary to the winter, the summer columns are more uniform from one year to another with values around 2.1x10^{16} to 2.8x10^{16} molec.cm^{-2}."* (p. 7 line 8-11)

42) p6, L21: I assume that "Cst" in Eqn (1) is a constant term, but it should be defined

Indeed, it is. This was added in the definition of the various terms (p. 7 line 19).

43) p6, L29: Kyrola et al. [2010] seems like an odd reference for such a general statement about the BDC. Wouldn't the Butchart [2014] review paper (already cited elsewhere) be a better choice?

Absolutely, this is quite odd indeed. The reference was modified (p.7 line 26).

44) p7, L13: further –> below

The word "further" was replaced by "below" (p. 8 line 11).

45) p7, L19: ENSO should also be mentioned here

The ENSO was added: *"… and geophysical proxies for the solar cycle, the QBO, the ENSO phenomenon and for the Arctic (AO) and Antarctic Oscillations (AAO) for the northern and southern hemispheres, respectively."* (p. 8 line 16-18)

46) p8, L13: meridonal –> meridional

The word was corrected (p. 9 line 13).

47) p8, L23: I assume it is meant that AO/AAO are considered only in the high latitudes of the hemisphere they are related to, since they are both applied in equatorial regions.

That is correct. To avoid any confusion, a precision was added: *"Each index (AO or AAO) is considered only in the hemisphere it is related to, …"* (p. 9 line 23)

48) p8, L29: delete "(from 195 K or TNAT for the formation of nitric acid trihydrate particles)"

The parenthesis was deleted (p.9 line 29).

49) p8, L30: "PSCs" has already been defined

Only the acronym was used (p.9 line 29).

50) p8, L31: delete "either"

The word was removed (p.9 line 30).

51) p9, L2: NAT has already been defined

Only the acronym was used (p.10 line 1).

52) p9, L3: gaz –> gas

The spelling was corrected (p.10 line 2).

53) p9, L13: dynamic –> dynamics

The word was corrected (p. 10 line 12).

54) p9, L23: Section 3.2 –> Section 4.2

The number of the section was changed (p. 10 line 22).

55) p9, L26: add "bands" after "90S"

The word "bands" was added (p. 10 line 25).

56) p9, L29: add "major" after "Most"

The word "major" was added (p. 10 line 28).

57) p9, L30: RMSE is used here for the first time but not defined until p11, L31

RMSE was defined here and only the acronym is used further (p. 10 line 29-30).

58) p10, L6: denitrifications –> denitrification seasons

The phrasing was modified (p.11 line 6).

59) p10, L11: delete "here"

The word "here" was removed (p. 11 line 12).

60) p10, L17: better –> improved

The word “better” was replaced by “improved” (p. 11 line 18).

61) p10, L23: dynamic –> conditions

The word “dynamic” was replaced by “conditions” (p. 11 line 25).

62) p11, L5: The reference to Section 4.4.1 is incorrect (this part of the discussion is itself in Section 4.4.1)

Indeed, we are referring to the first feature that is described in this section. The reference was changed to: *“(see first highlighted feature above)”.* (p. 12 line 7)

63) p11, L11: most –> much; also add “generally” in front of “between”

The word “most” was replaced by “much”. “generally” was added in front of “between” (p. 12 line 13)

64) p11, L19: between –> in

The word “between” was replaced by “in”. (p. 12 line 22)

65) p11, L21: emitted –> produced

The word “emitted” was replaced by “produced” (p. 12 line 23).

66) p11, L25: oxydation –> oxidation

The spelling was corrected (p. 12 line 29).

67) p11, L34: desertic –> desert

The word was corrected (p. 13 line 3).

68) p12, L30: For MEI, “south of Africa” the results are not significant. I think “west of South Africa” would be better here.

Indeed there was some confusion here. It was replaced by the suggested “west of South Africa”. (p. 14 line 16)

69) p13, L5: Groenland –> Greenland

The spelling was corrected (p. 14 line 21).

70) p13, L10: largely –> strongly

The word “largely” was replaced by “strongly” (p. 14 line 26).

71) p13, L21: further –> subsequent

The word “further” was replaced by “subsequent” (p. 15 line 9).

72) p13, L25: add “proxy” after “VPSC” and “HNO3” in front of “variability”

The word “PSCs” was used instead of “VPSC” (p. 15 line 13).

73) p14, L7: reveal –> reflect

The word “reveal” was replaced by “reflect” (p. 15 line 28).

74) p14, L14: between –> in

The word “between” was replaced by “in” (p. 16 line 3).

75) p14, L23: but still allow improving significantly the model-to-observation agreement –> but accounting for PSCs still significantly improves the model-to-observation agreement

The sentence was adapted as suggested (p. 16 line 11-12).

Spatio-temporal variations of HNO_3 total ~~column~~ columns from 9 years of IASI measurements - A driver study

Gaétane Ronsmans[1], Catherine Wespes[1], Daniel Hurtmans[1], Cathy Clerbaux[1,2], and Pierre-François Coheur[1]

[1]Université Libre de Bruxelles (ULB), Faculté des Sciences, Chimie Quantique et Photophysique, Brussels, Belgium
[2]LATMOS/IPSL, UPMC Univ. Paris 06 Sorbonne Universités, UVSQ, CNRS, Paris, France

Correspondence to: Gaétane Ronsmans (gronsman@ulb.ac.be)

Abstract. This study aims at understanding the spatial and temporal variability of HNO_3 total columns in terms of explanatory variables. To achieve this, multiple linear regressions are used to fit satellite-derived time series of HNO_3 daily averaged total columns. First, an analysis of the IASI 9-year time series (2008-2016) is conducted based on various equivalent latitude bands. The strong and systematic denitrification of the southern polar stratosphere is observed very clearly. It is also possible to distinguish, within the polar vortex, three regions wich are differently affected by the denitrification. Three exceptional denitrification episodes in 2011, 2014 and 2016 are also observed in the northern hemisphere, due to unusually low arctic temperatures. The time series are then fitted by multivariate regressions to identify what variables are responsible for HNO_3 variability in global distributions and time series, and to quantify their respective influence. Out of an ensemble of proxies (annual cycle, solar flux, quasi-biennial oscillation, multivariate ENSO index, Arctic and Antarctic oscillations and volume of polar stratospheric clouds), only the ones defined as significant (p-value < 0.05) by a selection algorithm are retained for each equivalent latitude band. Overall, the regression gives a good representation of HNO_3 variability, with especially good results at high latitudes (60-80% of the observed variability explained by the model). The regressions show everywhere the dominance of the annual variability, which is related to specific chemistry and dynamic depending on the latitudes. We find that the ~~PSCs~~ polar stratospheric clouds (PSCs) also have a major influence in the polar regions, and that their inclusion in the model improves the correlation coefficients and the residuals. However, there is still a relatively large part of the HNO_3 variability that remains unexplained by the model, especially in the intertropical regions, where factors not included in the regression model (such as vegetation fires or lightning) may be at play.

1 Introduction

Nitric acid (HNO_3) is known to influence the ozone (O_3) concentrations in the polar regions, because of its role of NO_x ($\equiv NO+NO_2$) reservoir and its ability to form polar stratospheric clouds (PSCs) inside the vortex ~~(Solomon, 1999; Urban et al., 2009; Popp~~ Solomon (1999); Urban et al. (2009); Popp et al. (2009)). In the stratosphere, HNO_3 forms from the reaction between OH and NO_2 (produced by the reaction N_2O+O^1D) and is destroyed by its reaction with OH or its photodissocation, both of these reactions being slow in daytime and virtually ~~inexsitent~~ non-existent during nighttime (McDonald et al., 2000; San-

tee et al., 2004). This leads to photochemical lifetimes between 1 and 3 months up to 30 km altitude and around 10 days above (Austin et al., 1986), inducing similar transport pathways for O_3 and NO_y (the sum of all reactive nitrogen species, i.e. including HNO_3) in general (Fischer et al., 1997). During the polar winter, with the arrival of low temperatures, ~~polar stratospheric clouds (PSCs)~~PSCs, composed of HNO_3, sulphuric acid (H_2SO_4) and water ice (H_2O), form within the vortex ~~(Voigt et al., 2000; von König et al., 2002).~~(e.g. Voigt et al. (2000); von König et al. (2002)). They act as sites for heterogeneous reactions, turning inactive forms of chlorine and bromine into active radicals, and leading to the depletion of O_3 in the polar regions ~~(Solomon, 1999; Wang and Michelangeli, 2006; Harris et al., 2010; Wegner et al., 2012).~~(e.g. Solomon (1999); Wang and Mich
Furthermore, the formation of these PSCs, and particularly of the nitric acid trihydrates (NAT), leads to a denitrification of the stratosphere (condensation of HNO_3 ~~and further~~ followed by sedimentation towards the lower stratosphere), which prevents $ClONO_2$ to reform ~~(Gobbi et al., 1991; Solomon, 1999; Ronsmans et al., 2016)~~ (e.g. Gobbi et al. (1991); Solomon (1999); Ronsmans et al.
and enhances further the depletion of ozone.

HNO_3 was measured by a variety of instruments in the last decades, amongst which the ~~Microwave Limb Sounder (MLS ,~~ MLS (on the UARS, then the ~~AURA~~ Aura satellite) provided the most complete data set. Its measurements started in 1991 and allowed extensive analyses on the seasonal and interannual variability, as well as on the vertical distribution of HNO_3 (Santee et al., 1999, 2004), with however a coarse horizontal resolution. Other instruments have also measured HNO_3 in the atmosphere, such as MIPAS (ENVISAT, Piccolo and Dudhia (2007)), ACE-FTS (SCISAT, Wang et al. (2007)) and SMR~~(ODIN~~[1] (Odin, Urban et al. (2009)), but few of these data have been used for geophysical analyses in terms of chemical and physical processes influencing HNO_3, mostly because of the limited horizontal sampling of these instruments.

On the other hand, O_3 has been extensively analysed, and numerous studies have been conducted to provide a better understanding of the factors influencing the stratospheric O_3 depletion processes and to assess the efficiency of the international treaties that were put in place to reduce its extent ~~(Lary, 1997; Solomon, 1999; Morgenstern et al., 2008; Mäder et al., 2010; Knibbe et al., 2014; W~~ Lary (1997); Solomon (1999); Morgenstern et al. (2008); Mäder et al. (2010); Knibbe et al. (2014); Wespes et al. (2016)). Most recent studies have used multivariate regression analyses in order to identify and quantify the main contributors to the O_3 spatial and seasonal variations. The variables included in such regression models depend on the atmospheric layer investigated (troposphere or stratosphere) and most often include the solar cycle, the quasi-biennial oscillation (QBO), the aerosol loading and the equivalent effective stratospheric chlorine (EESC) ~~(Wohltmann et al., 2007; Sioris et al., 2014; de Laat et al., 2015).~~(e.g. Wohltmann et al. (2007); Sioris et al. (2014); de Laat et al. (2015)). They often also include climate-related proxies for specific dynamical patterns such as El Niño southern oscillation (ENSO), the North Atlantic Oscillation (NAO) or the Antarctic Oscillation (AAO) (Frossard et al., 2013; Rieder et al., 2013). ~~Most often, the multivariate regression analyses use~~ In various multivariate regression studies, an iterative selection procedure is used to isolate the relevant variables for the concerned species ~~(Mäder et al., 2007)~~(Steinbrecht, 2004; Mäder et al., 2007; Knibbe et al., 2014; Wespes et al., 2016, 2017).

Despite the fact that it is one of the main species influencing stratospheric O_3, HNO_3 has much less been studied in terms of explanatory variables, in part because of the lack of global, consistent and sustained measurements. Identifying the factors

[1] in the order of the instruments cited above: Microwave Limb Sounder, Michelson Interferometer for Passive Atmospheric Sounding, Atmospheric Chemistry Experiment-Fourier Transform Spectrometer, Sub-Millimetre Radiometer

driving its spatial and temporal variability could help to characterize its behaviour in the stratospheric chemistry, and hence its interactions with O_3.

The Infrared Atmospheric Sounding Interferometer (IASI) onboard the Metop satellites has been and still is providing global measurements of the HNO_3 total column, which are used here to investigate the HNO_3 spatial and temporal variability. The data set used (Section 2) consists of time series of HNO_3 columns retrieved from IASI/Metop A measurements over the period 2008-2016, twice daily and with global coverage. The unprecedented spatial and temporal sampling of the high latitudes allows for an in-depth monitoring of the atmospheric state in particular during the polar winter (Wespes et al., 2009; Ronsmans et al., 2016). We make use of equivalent latitudes in order to isolate polar air masses with specific polar vortex characteristics, and hence to better understand the role of HNO_3 in the polar chemistry, with regard to geophysical features such as the extent of the polar vortex and polar temperatures (Section 3). We next apply multivariate regressions to the IASI-derived HNO_3 time series to statistically characterize their global distributions and seasonal variability for the first time, and this at different latitudes. The global coverage and the sampling of observations also allow retrieving global patterns of the main HNO_3 drivers (Section 4).

2 IASI HNO_3 data

The HNO_3 columns used here were retrieved from the measurements of the IASI instrument onboard the Metop A satellite. IASI measures the upwelling infrared radiation from the Earth's surface and the atmosphere in the 645-2760 cm^{-1} spectral range at nadir and off nadir along a broad swath (2200 km). The level 1C data set used for the retrieval consists of ~~bi-daily measurements~~ measurements taken twice a day (at 9:30 AM and PM, equator crossing time) at a 0.5 cm^{-1} apodized spectral resolution and with a low radiometric noise (0.2 K in the HNO_3 atmospheric window) (Clerbaux et al., 2009; Hilton et al., 2012). The ground field of view of the instrument consists of 4 elliptical pixels (2 by 2) yielding a horizontal footprint (single pixel) that varies from 113 km^2 (12 km diameter) at nadir to 400 km^2 at the end of the swath.

To retrieve HNO_3 atmospheric concentrations, we use the level 1C measurements available in near-real time at ~~ULB~~ Université Libre de Bruxelles (ULB) and retrieved by the Fast Optimal Retrievals on Layers for IASI (FORLI) software, which uses the optimal estimation method (Rodgers, 2000). A complete description of the FORLI method can be found in Hurtmans et al. (2012) and a summary of the retrieval parameters specific to HNO_3 in Ronsmans et al. (2016). The retrieval initially yields HNO_3 vertical profiles on 41 levels (from 0 to 40 km altitude) but with limited vertical sensitivity. The characterization of the retrieved profiles conducted by Ronsmans et al. (2016) showed indeed that the degrees of freedom for signal (DOFS) range from 0.9 to 1.2 at all latitudes. Because of this lack of vertical sensitivity, the HNO_3 total column is the most representative quantity for the IASI measurements and it is exploited here for the investigation of the HNO_3 time evolution. It is important to note, however, and as thoroughly discussed ~~by~~ in Ronsmans et al. (2016), that the information on the HNO_3 profile comes mostly from the ~~low-middle~~ lower stratosphere (15-20 km) and that the profile is therefore mainly indicative of the stratospheric abundance. In order to compute the total column, the retrieved vertical profiles are integrated over the whole altitude range. Our previous study showed that the resulting total columns yield a mean error of 10% and a low bias (10.5%) when compared to ground-based FTIR measurements (Ronsmans et al., 2016). The data set used spans from January 2008 to December 2016

with daily median HNO_3 columns averaged on a $2.5° \times 2.5°$ grid, for which both day and night measurements were used. Based on cloud information from the EUMETSAT operational processing, the cloud-contaminated scenes are filtered out, i.e. all scenes with a ~~higher~~ fractional cloud cover higher than 25% are not taken into account. It should be noted that there was an abnormally small amount of IASI L2 data distributed by EUMETSAT between the 14th of September and the 2nd of December 2010 (Van Damme et al., 2017), and that these data have been removed from the figures and analyses in the following of the paper. For the present study, the data are divided into several time series according to equivalent latitudes (sometimes here referred to as "eqlat") which allow to consider dynamically consistent regions of the atmosphere throughout the globe and to better preserve the sharp gradients across the edge of the polar vortex. The potential vorticity data are daily fields obtained from ECMWF ERA Interim reanalyses, taken at the potential temperature of 530 K. Following the analysis of the potential vorticity contours, we consider 5 equivalent latitude bands in each hemisphere (30°-40°, 40°-55°, 55°-65°, 65°-70°, 70°-90°), plus the intertropical band (30°N - 30°S), with the corresponding potential vorticity contours, in units of $\times 10^{-6}$ $K.m^2.kg^{-1}.s^{-1}$, being at 2.5 (30°), 3 (40°), 5 (55°), 8 (65°) and 10 (70°) (Figure 1).

3 HNO_3 time series

The HNO_3 time series for the mid to high latitudes are displayed in Figure 2 for the years 2008-2016. Total columns are represented for both north (green) and south (blue curves) hemispheres, for equivalent latitudes bands 40-55°, 55-65°, 65-70°and 70-90°. Also highlighted by shaded areas are the periods during which the southern and northern polar temperatures, taken at 50 hPa (light blue and light green for the 70-90 eqlat band, S and N respectively, and purple for the 65-70 S eqlat band), were equal to or below the polar stratospheric clouds formation threshold (195 K, based on ECMWF temperatures). It should be noted that ~~this temperature corresponds to~~ while this temperature is a widely accepted approximation for the formation threshold for NAT (type I), ~~but that~~ its actual value can be different depending on the local conditions (Lowe and MacKenzie, 2008; Drdla and Müller, 2010; Hoyle et al., 2013). Also, other forms of PSCs, particularly the type II PSCs (ice clouds) form at a lower temperature of 188 K~~(Santee et al., 1999; Wespes et al., 2009).~~, corresponding to the frostpoint of water, or 2-3 K below that (e.g. Toon et al. (1989); Peter (1997); Tabazadeh et al. (1997); Finlayson-Pitts and Pitts (2000)).

As a general rule, we find larger concentrations in the northern hemisphere, for the entire latitude range shown here (40-90 eqlat). The hemispheric difference in HNO_3 maximum concentrations can be partly attributed to the hemispheric asymmetry of the Brewer-Dobson circulation associated with the many topographical features in the northern hemisphere compared to the southern hemisphere. As a result, the northern hemisphere has a more intense planetary wave activity, which strengthens the deep branch of the Brewer-Dobson circulation. This has also a direct effect on the latitudinal mixing processes, which usually extend into the Arctic polar region, but less into the Antarctic due to a stronger polar vortex (Mohanakumar, 2008; Butchart, 2014).

~~Further than~~ Beyond the hemispheric asymmetry, we also find that the HNO_3 columns are generally larger at higher latitudes, with total column maxima between 3.0×10^{16} and 3.7×10^{16} molec.cm^{-2} in the equivalent latitudes bands 70-90°, 65-70° and 55-

65°, and lower at around 2.2×10^{16} molec.cm^{-2} in the 40-55° band, especially for the southern hemisphere. This latitudinal gradient of HNO_3 ~~columns~~ has been previously documented ~~(Santee et al., 2004; Urban et al., 2009; Wespes et al., 2009; Ronsmans et al., 201~~ Santee et al. (2004); Urban et al. (2009); Wespes et al. (2009); Ronsmans et al. (2016)) and can be explained mainly by the larger amounts of NO_y at high latitudes due to a larger age of air and by the NO_y partitioning favoring HNO_3. Another interesting feature observable in Figure 2 is the different behaviour of the three highest latitude regions with regard to the polar stratospheric clouds formation threshold in the southern hemisphere. The denitrification process that occurs with the condensation and sedimentation of PSCs (see e.g. Wespes et al. (2009); Manney et al. (2011) and Ronsmans et al. (2016) for further details) is obvious in the 70-90 S region (top panel, blue curve in Figure 2), with a systematic and strong decrease in HNO_3 total columns (from 3.3×10^{16} to 1.5×10^{16} molec.cm^{-2}) starting within 12 to 25 days after the stratospheric temperature reaches the threshold of 195 K (start of the blue shaded areas). The ~~denitrification~~ loss of HNO_3 thus usually starts around the beginning of June in the Antarctic and the concentrations reach their minimum value within one month. They stay low at 1.4×10^{16} molec.cm^{-2} until mid-November (with quite often a slight gradual increase to 1.7×10^{16} molec.cm^{-2} during the two following months), and start to increase again during January, i.e. between 2.5 and 3 months after the polar stratospheric temperatures are back above the NAT formation threshold. The same pattern can be observed in the 65-70 S equivalent latitude region, with however, a delay of approximately 1 month for the start of the steepest decrease in HNO_3 columns, which appears to be more gradual than in the 70-90 S regions (3 months to reach the minimum values, starting in July). The minimum and plateau column values are thus reached by the end of September; they remain higher than at the highest latitudes, with values staying at around 1.7×10^{16} molec.cm^{-2}. The delayed and less severe ~~denitrification~~ loss of HNO_3 in the 65-70 S band confirms that the denitrification process spreads from the center of the polar vortex, where the lowest temperatures are reached first (McDonald et al., 2000; Santee et al., 2004; Lambert et al., 2016). This spreading from the center also leads to slightly higher concentrations for the maxima in the 65-70 S eqlat band (mean of maxima of 3.26×10^{16}, versus 3.11×10^{16} molec.cm^{-2} in the 70-90 S eqlat band). The delayed ~~denitrification in~~ decrease in HNO_3 in the outer parts of the vortex (i.e. in the 65-70 S eqlat band) can thus be attributed to the later appearance of PSCs in this region (see Figure 2 purple shaded areas in second panel)~~, and to the mixing of these air masses with the denitrified air masses from the center of the vortex~~. ~~These two processes lead to~~ By the end of December, i.e. when the vortex has started breaking down (e.g. Schoeberl and Hartmann (1991); Manney et al. (1999); Mohanakumar (2008)), the total columns in both eqlat bands ~~being in~~ homogenize and reach the same range of values ~~by the end of December~~ (1.7×10^{16} molec.cm^{-2}). If the decrease is slower at 65-70 eqlat, this is not the case for the recovery, with the build-up of concentrations that starts roughly at the same time as for the 70-90 S eqlat band, hence resulting in a shorter period of denitrified atmosphere in the 65-70 S band. These results agree well with previous studies by McDonald et al. (2000) and Santee et al. (2004) for earlier years. ~~As for the~~ However, the recovery of the HNO_3 total columns is very slow compared to other species, namely O_3, for which concentrations return rapidly to usual values almost as soon as PSCs disappear. In fact, the HNO_3 columns stay low well after the September equinox and are only subject to a slow increase 2 months later (in early December). While more persistent local temperature minima staying below 195 K could explain part of this late recovery, we make the hypothesis that it is due mainly to a combination of two factors: (1) a significant sedimentation of PSCs towards the lower atmosphere during the winter, yielding only small amounts of it

to release HNO_3 under warmer temperatures (Lowe and MacKenzie, 2008; Kirner et al., 2011; Khosrawi et al., 2016), and (2) the effective photolysis of HNO_3 and NO_3 in spring and summer under prolonged sunlight conditions, i.e. mainly at the highest latitudes, which respectively increase the HNO_3 sink and reduce the chemical source (because NO_3 cannot react with NO_2 to produce N_2O_5, Solomon (1999); Jacob (2000); McDonald et al. (2000)). The increase observed in March, at the start of the winter, is in turn explainable by a much reduced number of hours of sunlight, implying less photodissociation.

It is worth noting that the two regions previously mentioned (inner and outer vortex) have been observed to behave differently; the inner vortex (70-90 S) undergoes strong internal mixing whereas the outer vortex (65-70 S), isolated from the vortex core, experiences little mixing of air. This, combined to a cooling of the stratosphere, could lead to increased PSC formation and further ozone depletion (Lee et al., 2001; Roscoe et al., 2012).

Regarding the HNO_3 columns in the 55-65 S eqlat band, which comprises the vortex rim~~itself~~, or "collar" (Toon et al., 1989), it is evident from Figure 2, third panel, that it is not affected by denitrification, in agreement with previous observations (e.g. Santee et al. (1999); Wespes et al. (2009); Ronsmans et al. (2016)). In fact, we show that the columns in that band keep increasing ~~during the low-temperature periods~~ when the temperatures at higher latitudes start decreasing, to reach maximum values of about 3.4×10^{16} molec.cm^{-2} in June-July; this is due to a change in the NO_y partitioning towards HNO_3, itself due to less sunlight compared to ~~lower latitudes .~~ the summer. Also inducing increased concentrations during the winter at high latitudes is the diabatic descent occurring inside the vortex when the temperatures decrease. This downward motion of air enriches the lower stratosphere in HNO_3 coming from higher altitude (Manney et al., 1994; Santee et al., 1999), yielding higher column values which are, in this eqlat band, not affected by denitrification. The slow decrease starting in August and leading to minimum values in January is related to the combined effect of increased photodissociation and mixing with the denitrified polar air masses which are no ~~more~~ longer confined to the polar regions. Finally, as previously mentioned, the 40-55 S eqlat band records lower column values throughout the year (generally below 2×10^{16} molec.cm^{-2}) and a much less pronounced seasonal cycle.

The northern hemisphere high latitudes usually do not experience denitrification, mostly because the temperatures, while sometimes showing local minima below 195 K, rarely reach the PSC formation threshold on broad areas and for long time spans (see Figure 2 for average temperatures, light green vertical areas). A few years stand out, however, with exceptionally low stratospheric temperatures. This is especially the case of the 2011 (Manney et al., 2011), 2016 and, to some extent, 2014 Arctic winters. During these three winters, temperatures reached below the 195 K threshold over a broader area and stayed low during a longer period than usual. Lower concentrations of HNO_3 have been recorded in consequence, especially in the northernmost equivalent latitude band (see Figure 2). The winter 2016 recorded in particular exceptionally low temperatures and led to large denitrification and significant ozone depletion (Manney and Lawrence, 2016; Matthias et al., 2016). The denitrification that occurred in the northern polar regions affected a smaller area than what generally happens in the southern hemisphere; in particular the columns in the 65-70 N eqlat band do not show a significant decrease.

Figure 3, which consists in the time series of the zonally averaged distribution of the HNO_3 retrieved total columns, illustrates all these features particularly well: it highlights the low and constant columns between -40 and 40 degrees of latitude, the marked annual cycle at mid to high latitudes ~~,~~ and the systematic and the occasional (2011, 2014, 2016) ~~denitrification~~ loss of

HNO_3 during the denitrification periods in the high latitudes of the Southern and Northern hemispheres respectively, which are highlighted by the iso-contours of ~~polar vorticity at -10~~potential vorticity at $\pm$ 10$\times10^{-6}$ K.m^2.kg^{-1}.s^{-1} (dark blue).

In order to give further insights into the interannual variability in polar regions, Figure 4 shows the seasonal cycle for each individual year from 2008 to 2016 for eqlat 70-90 in the northern (top) and the southern (bottom) hemispheres. ~~It should be noted that there was an abnormally small amount of IASI L2 data distributed by Eumetsat between the 14th of September and the 2nd of December 2010 (Van Damme et al., 2017), and that these data have been removed from the Figure (see interrupted green curve).~~ July and August of 2010 ~~also~~ stand out in the Antarctic, with high and variable columns recorded by IASI. ~~Although we do not, at this stage, have a clear understanding of this, we hypothesize that this~~ This is a consequence of a mid-winter (mid-July) minor sudden stratospheric warming (SSW) event that induced a downward motion of air masses and modified the chemical composition of the atmosphere between 10 and 50 hPa ~~(de Laat and van Weele, 2011).~~ and until at least September (de Laat and van Weele, 2011; Klekociuk et al., 2011). The principal effect of this sudden stratospheric warming was to reduce the formation of PSCs (which stayed well below the 1979-2012 average (WMO, 2014)) and hence reduce denitrification. This is shown by an initial drop in June, as is usually observed in other years but then by an increase in HNO_3 columns when the SSW occurs. These results confirm those previously obtained by the Aura MLS during that winter and reported in the World Meteorological Organization (WMO) Ozone Assessment of 2014 (see Figure 6-3, WMO (2014)). Apart from these peculiarities for the year 2010, all years seem to coincide quite well in terms of seasonality in the southern hemisphere (bottom panel). The timing of the ~~denitrification is in particular~~ HNO_3 steep decrease in particular is consistent from one year to another.

The northern hemisphere high latitudes (top panel) show more interannual variability ~~especially~~ than in the south, especially during the winter because of the unusual ~~dentrification~~ denitrification periods observed in 2011 (purple), 2014 (blue) and 2016 (black) in January (concentrations as low as 2.2$\times10^{16}$ molec.cm^{-2} in 2016)~~, during the summer, the~~ . Contrary to the winter, the summer columns are more ~~stable~~ uniform from one year to another with values around 2.1$\times10^{16}$ to 2.8$\times10^{16}$ molec.cm^{-2}.

4 Fitting the observations with a regression model

4.1 Multi-variable linear regression

In order to identify the processes responsible for the HNO_3 variability observed in the IASI measurements, we use a multivariate linear regression model featuring various dynamical and chemical processes known to affect HNO_3 distributions. We follow strictly the methodology set-up by Wespes et al. (2016) for similarly investigating the O_3 variability. In particular, as in Wespes et al. (2016), we use daily median HNO_3 total columns. These are fitted with the following model:

$$\mathrm{HNO_3}(t) = cst + y_1.trend + [a_1.cos(\omega t) + b_1.sin(\omega t)] + \sum_{i=2}^{m}[y_i.Y_{\mathrm{Norm,i}}(t)] + \epsilon(t) \quad (1)$$

where t is the day in the time series, *cst* is a constant term, the y terms are the regression coefficients for each variable, $\omega = 2\pi/365.25$, and $Y_{\mathrm{Norm,i}}(t)$ refer to the chosen explanatory variables Y, which are normalized over the period of IASI

observations (2008-2016) following:

$$Y_{\text{Norm,i}}(t) = 2(Y(t) - Y_{\text{median}})/(Y_{\text{max}} - Y_{\text{min}}) \quad (2)$$

with Y_{max} and Y_{min} the maximum and minimum values of the variable time series (before subtraction of the median, Y_{median}). The terms a_1 and b_1 in Eq.(1) are the coefficients accounting for the annual variability in the atmosphere. They account mainly for the seasonality of the solar insolation and of the meridional Brewer-Dobson circulation, which is a slow stratospheric circulation redistributing the tropical air masses to extra-tropical regions ~~(Mohanakumar, 2008; Kyrölä et al., 2010)~~(Mohanakumar, 2008; Butch

The regression coefficients are estimated by the least squares method. The standard error (σ_e) of each proxy is calculated based on the regression coefficients and is corrected in order to take the autocorrelation uncertainty into account (Knibbe et al., 2014; Wespes et al., 2016):

$$\sigma_e{}^2 = (\mathbf{Y}^T\mathbf{Y})^{-1} \cdot \frac{\sum[\text{HNO}_3 - \mathbf{Y}y]^2}{n-m} \cdot \frac{1+\varphi}{1-\varphi} \quad (3)$$

where $\mathbf{Y}$ is the matrix of explanatory variables of size $n \times m$, n is the number of daily measurements and m the number of fitted parameters. HNO_3 is the nitric acid column, y the vector of regression coefficients and φ is lag-1 autocorrelation of the residuals.

4.2 Iterative selection of explanatory variables

The choice of variables included in the model is made using an iterative elimination procedure; all variables are tested based on their importance for the regression (Mäder et al., 2010). At each iteration, the variable with the largest p-value (and outside the confidence interval of 95%) is removed, until there remain only the variables relevant for the regression, i.e. the ones with a p-value smaller than 0.05. This selection algorithm is applied on each band of equivalent latitude (or grid cell, for the global distributions shown ~~further~~below) and thus yields a different combination of variables, depending on the equivalent latitude region considered.

4.3 Variables used for the regression

Given the strong relationship between the O_3 and the HNO_3 chemistry and variability (Solomon, 1999; Neuman et al., 2001; Santee et al., 2005; Popp et al., 2009) and the novelty in applying such a regression study in an HNO_3 dataset, we consider here the major and well known drivers of the total O_3 variability, namely: a linear trend, harmonic terms for the annual variability and geophysical proxies for the solar cycle, ~~for the QBO~~the QBO, the ENSO phenomenon and for the Arctic (AO) and Antarctic Oscillations (AAO) for the northern and southern hemispheres, respectively. Considering the short length of the time series, however, the linear trend did not yield any significant result and, recalling that the aim of the paper is not to derive long term trends, this aspect will not be discussed further. In addition, a proxy for the volume of polar stratospheric clouds is included to

account for the effect of the strong denitrification process during the polar night (cf. Section 3). All the proxies are shown in Figure 5 and described with more details hereafter. The source for each proxy is also provided in Table 1.

4.3.1 Solar flux (SF)

As a proxy for the solar activity, we use the 10.7 cm solar flux ($F_{10.7}$). It is a radio flux that varies daily, and correlates to the number of sunspots on the solar disk (Covington, 1948; Tapping and DeTracey, 1990; Tapping, 2013). The data set used here is the adjusted flux that takes the changing earth-sun distance into account. The solar cycle influences directly the partitioning between NO_y (produced by the N_2O+O^1D reaction) and HNO_3 through the quantity of sunlight available, and has been known to affect the dynamics and to influence the O_3 response in the lower stratosphere ~~(Hood, 1997; Kodera and Kuroda, 2002; Hood and Soukharev~~ Hood (1997); Kodera and Kuroda (2002); Hood and Soukharev (2003); Austin et al. (2007)).

4.3.2 Quasi-Biennial Oscillation (QBO)

The QBO is one of the main process regulating the dynamics of the tropical atmosphere ~~(Baldwin et al., 2001; Sioris et al., 2014).~~(e.g. Baldwin et al. (2001); Sioris et al. (2014)). It is driven by vertically propagating gravity waves, which lead to an oscillation between stratospheric winds blowing from east (easterlies) and from west (westerlies), with a period of about 28-29 months ~~(Hauchecorne et al., 2010; Schirber, 2015).~~(e.g. Hauchecorne et al. (2010); Schirber (2015)). Its effect on the distribution of chemical species is significant, especially in equatorial regions where both a direct effect due to the changing winds and an indirect effect via its influence on the Brewer-Dobson circulation, affect, for example, the distribution of ozone ~~(Lee and Smith, 2003; Mohanakumar, 2008; Frossard et al., 2013; Knibbe et al., 2014).~~(e.g. Lee and Smith (2003); Mohanakumar (2008);
Two monthly time series of QBO at two different pressure levels (30 hPa and 10 hPa) from ground-based measurements in Singapore have been considered for the present study, in order to take into account the differences in phase and shape of the QBO signal in the upper and lower stratosphere.

4.3.3 Multivariate ENSO Index (MEI)

The Multivariate ENSO Index is a metric that quantifies the strength of the El Niño-Southern Oscillation; it is computed based on the measurement of six variables over the tropical Pacific: sea-level pressure, zonal and ~~meridonal~~ meridional winds, sea surface temperature, surface air temperature and cloudiness fraction (Wolter and Timlin, 1993, 1998). The ENSO phenomenon, even though it is a tropospheric process (mainly sea surface temperature contrasts), also affects stratospheric circulation. Previous studies have shown the impact of El Niño/La Niña oscillation on the stratospheric transport processes and the generation of Rossby waves, in turn modulating the strength of the polar vortex ~~(Trenberth et al., 1998; Newman et al., 2001; Garfinkel et al., 2015)~~ (e.g. Trenberth et al. (1998); Newman et al. (2001); Garfinkel et al. (2015)) and affecting O_3 in the stratosphere ~~(Randel et al., 2009; Lee et al., 2~~ Randel et al. (2009); Lee et al. (2010); Randel and Thompson (2011)).

4.3.4 Arctic Oscillation and Antarctic Oscillation

The ~~Arctic (AO) and Antarctic Oscillations (AAO)~~ AO and AAO are included in the regression in order to represent the atmospheric variability observed in the northern and southern hemispheres, respectively (Gong and Wang, 1999; Kodera and Kuroda, 2000; Tho
They are constructed from the daily geopotential height anomalies in the 20-90° region, at 1000 mb (for the northern hemisphere) and 700 mb (for the southern hemisphere). Each index (AO or AAO) is considered only in the hemisphere it is related to, while both indices are included for equatorial latitudes. The impact of these oscillations on O_3 distributions has been demonstrated in several studies ~~(Rieder et al., 2013; Wespes et al., 2016).~~(e.g. Rieder et al. (2013); Wespes et al. (2016)). We may expect similar influence on the HNO_3 distributions, particularly because, even though they are tropospheric features, their phase and intensity affect the atmospheric circulation, and in particular the Brewer-Dobson Circulation, up to the stratosphere (Miller et al., 2006; Chehade et al., 2014).

4.3.5 Volume of Polar Stratospheric Clouds (VPSC)

The very low temperatures recorded during the winter in the polar stratosphere inside the vortex lead ~~(from 195 K or T_{NAT} for the formation of nitric acid trihydrate particles)~~ to the formation of ~~polar stratospheric clouds (PSCs)~~PSCs, which are composed ~~either~~ of nitric acid di- or trihydrates (NAD or NAT), supercooled ternary $HNO_3/H_2SO_4/H_2O$ solutions (STS) or water ice (H_2O) ~~(Wang and Michelangeli, 2006; Drdla and Müller, 2010).~~(e.g Wang and Michelangeli (2006); Drdla and Müller (2010)).
Here, we consider for the PSCs only the ~~nitric acid trihydrate (NAT)~~ NAT particles ($HNO_3.(H_2O)_3$), which are ubiquitous (and often mixed with STS) (Voigt et al., 2000; Pitts et al., 2009; Lambert et al., 2016). The other forms of PSCs are expected to influence the variability in ~~gaz-phase~~ gas-phase HNO_3 to a much lesser extent (von König et al., 2002).
The proxy we use here for the NAT is the volume of air below T_{NAT} (195 K), which depends on nitric acid concentrations, water vapor and pressure (Hanson and Mauersberger, 1988; Wohltmann et al., 2007). The temperatures needed to compute that quantity are based on ERA-Interim reanalyses and the HNO_3 and H_2O profiles are taken north and south of 70° from an MLS climatology. The proxy is calculated with a supersaturation of HNO_3 over NAT of 10, roughly corresponding to 3K supercooling (Hoyle et al., 2013; Lambert et al., 2016; Wohltmann et al., 2017). It should be noted that this proxy was not included in the regression outside of the polar regions. Inside the polar regions (eqlat bands 70-90 north and south), it was included and subject to the selection algorithm.

Finally, it is worth to note that, for the sake of completeness, proxies accounting for the potential vorticity (PV) and for the Eliassen-Palm flux (EPflux) were also tested in order to take into account more precise patterns of the stratospheric ~~dynamic~~ dynamics and the Brewer-Dobson circulation. Also, various levels for the QBO were tested. However, none of these proxies lead to a significant improvement of the residuals or the correlation coefficients, and their signal is therefore embedded here in the harmonic terms. For these reasons, they will not be discussed further.

4.4 Results

The results are presented in two ways: first, latitudinally averaged time series (eqlat bands) are used to analyze the performances of the fit in terms of correlation coefficients and residuals, with a focus on polar regions. The performance of the model is then analysed in terms of global distributions (with the regression applied to every $2.5° \times 2.5°$ grid cell) and the spatial distribution of the fitted proxies is detailed.

4.4.1 HNO_3 fits for equivalent latitudes bands

For each eqlat band, the variables retained by the selection procedure (see Section ~~3.2~~ 4.2) are listed in Table 2. Most variables are retained everywhere, except for the solar flux which is rejected in the polar latitudes (70-90 N and S). The QBO30 is also excluded in the southern polar regions (65-90 S) and the MEI in the northern polar regions (65-90 N). Finally, the AO and AAO are excluded in the 65-70 N and in the 70-90 S bands, respectively.

The results from the multivariate regression are presented in Figure 6 for each band of equivalent latitude. The model reproduces well the measurements, with correlation coefficients between 0.81 (in the 30-40 N eqlat band) and 0.94 (in the 70-90 S eqlat bands). Most major features (seasonal and interannual variabilities) are reproduced by the regression model. The residuals range between 1.74×10^{10} and 9.44×10^{15} molec.cm^{-2}, with better results for the 30N-30S equivalent latitude band (~~RMSE~~ Root Mean Square Error (RMSE) of 2.39×10^{14} molec.cm^{-2}) and worse fits for the 65-70 S band (RMSE of 2.41×10^{15} molec.cm^{-2}). Following the comparison between the fits and the observational data, some features can be highlighted:

- The high daily variability recorded in the data during the winter for both polar regions is not captured very well by the regression fit. Indeed, we find that the residuals are largest in this period, especially in the southern hemisphere during the denitrification period of each year (from June until September approximately), mostly because of the high variability of the vortex itself. There, we find an average standard deviation of 1.44×10^{16} molec.cm^{-2} (average of the standard deviation during the denitrification periods over the 8 years of observation), as opposed to a mean standard deviation of 8.30×10^{15} molec.cm^{-2} for the periods between the ~~denitrifications~~denitrification seasons. In the northern hemisphere, the day-to-day variability is largest during winter as well, when the vortex builds up, and this causes larger residuals for the corresponding months (see December through March of each year, top left panel of Figure 6, with an average standard deviation of 7.97×10^{15} molec.cm^{-2} to be compared to 7.26×10^{15} molec.cm^{-2} for the other months). It is important to stress that these larger residuals are obtained in the polar regions despite the fact that a VPSC proxy was used. In Figure 7 we show, however, that the regression model would perform worse in polar regions if that proxy is neglected, as also discussed ~~here~~ below.

- Even though the high variability during the denitrification periods is not reproduced exactly, the amplitude of the decrease in HNO_3 occurring in the Southern polar region is captured accurately by the regression model. Figure 7 shows a zoom of Figure 6 to better highlight the model performance during the denitrification periods; the regression was tested without (top panels) and with (middle panels) the VPSC proxy, for the 70-90 N (left panels) and the 70-90 S (right panels) eqlat bands. The steep slope observed at the start of the low temperatures is captured by the model when the proxy for the

VPSC is included (Figure 7) and the correlation coefficients are improved for both hemispheres (from 0.83 to 0.86 in the 70-90 N and from 0.84 to 0.94 in the 70-90 S eqlat band). In the 65-70 S eqlat band however, as previously described in Section 3, the HNO_3 columns continue to increase after the formation of PSCs has started in the 70-90 S eqlat band. This translates to a lag between the observations in the 65-70 S eqlat band and the fit in which the drop of HNO_3 concentrations happens earlier than in the IASI observations. This is explained by the fact that the VPSC proxy is based on temperatures and composition poleward of 70°. It induces a lower correlation coefficient (0.87) and higher RMSE (2.41×10^{15} molec.cm^{-2}). A proxy adapted to this eqlat band should be used in further studies in order to represent the conditions in that particular region of the vortex.

– The high maxima seen in the IASI time series, mostly from mid-April through the end of May in the Southern hemisphere, and from mid-December through early February in the Northern hemisphere, are not that well reproduced by the regression model. In fact, the model fails to capture the highest columns during the winters of each hemisphere. In the same way, a few pronounced lows recorded by IASI, especially those in the Northern polar regions (mid-June to early October 2014 and 2016, for instance) are not captured by the model.

Figure 8 shows the regression coefficients of each variable in each equivalent latitude band (top panel). The two bottom panels show the signal of the fitted proxies, calculated by multiplying the proxy by its regression coefficient. Only the variables retained by the selection algorithm are shown and discussed. From the top panel of Figure 8, it can be seen that all proxies are significant, with errors smaller than the coefficients for all eqlat bands. It is clear that the annual variability is predominant at all latitudes. From the two bottom panels, we also see the large influence of the VPSC in the regression for the polar regions. Their signal is, as expected, larger in the southern hemisphere where it reaches -1.3×10^{16} molec.cm^{-2}, which is to be compared to maximum values around -0.4×10^{16} molec.cm^{-2} in the northern hemisphere. A noteworthy difference is found for the year 2016 where the VPSC signal reached -0.7×10^{16} molec.cm^{-2} during the exceptionally cold Arctic winter. While the PSCs have significantly affected the HNO_3 distributions in the winters 2011, 2014 and 2016 in the Arctic, their influence during other years may contribute to the high variability recorded in the observations (see ~~Section 4.4.1~~first highlighted feature above). Other proxies show relatively large signals and their global distribution will be discussed further in Section 4.4.3.

4.4.2 Global model assessment with regard to the HNO_3 variability

To assess the model ability to reproduce the measurements, the top panel of Figure 9 shows the percentage of the HNO_3 variability seen by IASI that is explained by the regression model. The fraction is calculated as the difference between the standard deviation of the fit and of the observations [σ ($HNO_3{}^{fit}$(t))/ σ ($HNO_3{}^{IASI}$(t)) $\times$ 100] and is expressed as a percentage. We find that ~~most~~ much of the observed variability can be explained by the model in the southern hemisphere (generally between 50 and 80 %). The southern mid-latitudes and the polar regions are in particular well modeled (70-80 %), except in Antarctica above the ice shelves. The northern hemisphere HNO_3 variability is reasonably well explained by the model, particularly above 40° of latitude, with percentages ranging between 50 and 80 %, although some continental areas (Northern

part of inner Eurasia above Kazakhstan and the west Siberian plains) stand out with percentages below 40 %. The region with the largest unexplained fraction of variability is the intertropical band extending as far as 40° north. There, the fraction of HNO_3 variability explained by the model reaches values as low as 20 %. These regions of low explained variability coincide quite well with the regions where a high lightning activity is found, which produces large amount of NO_x in the troposphere (Labrador et al., 2004; Sauvage et al., 2007; Cooper et al., 2014). While the IASI instrument is usually not sensitive to tropospheric HNO_3, it was found that large amounts of tropospheric HNO_3 ~~between~~ in the tropics could be detected, mainly because of the lower contribution of the stratosphere in that region, and because the NO_x ~~emitted~~ produced by lightning are released in the high troposphere, where IASI has still reasonable sensitivity. This could thus explain why the model is missing some of the variability recorded in the observational data. Another cause for the discrepancies between the observations and the model could be unaccounted sinks of HNO_3, such as deposition in the liquid or solid phase and scavenging by rain. It should be noted that a small area of high explained variability is observed in Africa, just south of the equator. The variability in this region is unexpectedly high in the IASI time series (Figure 10) and we suggest that it could be influenced by biomass burning emissions of NO_2, and subsequent ~~oxydation~~ oxidation to HNO_3 with a delay of about 2 months (Figure 10) (Scholes et al., 1996; Barbosa et al., 1999; Schreier et al., 2014). Indeed, the large vegetation fires of Africa every year around July emit the largest amounts of NO_x (compared to large fires of South America, Australia and southeast Asia). ~~If this hypothesis turns out to be true, it means that~~ Their influence translates to an overrepresentation of the annual term ~~, which carries this variability in the regression model , is overrepresented in the fitted model.~~ (up to -2×10^{15} molec.cm^{-2}) in the fitted model (although not clearly visible in Figure 11 because of the color scale chosen). This larger contribution of the annual variability thus yields a better agreement between the observations and the model in the tropical band, however missing some of the interannual variability due to these fires.

The bottom panel of Figure 9 depicts the global distribution of the ~~root mean square error (RMSE)~~ RMSE of the regression expressed as a percentage. The errors are small everywhere (between 10 and 20 %) except in the southern hemisphere above Antarctica, and particularly above the ice shelves (mainly the Ross and Ronne ice shelves). We also find higher values above the large ~~desertic~~ desert areas (the Sahara, the Arabian, the Turkestan and the Australian deserts) as well as off the west coasts of south Africa and South America where persistent low clouds occur. These regions of low clouds or characterized by sharp or seasonally varying emissivity features are known to cause problems for the retrieval of HNO_3 using the IASI spectra (Hurtmans et al., 2012; Ronsmans et al., 2016).

4.4.3 Global patterns of fitted parameters

Figure 11 shows the global distributions of the regression coefficients obtained after the multivariate regression, expressed in molec.cm^{-2}. All the variables are shown, with the areas where the proxy was not retained left blank. The contribution of each proxy to the HNO_3 variability was also calculated for each grid cell as $[\sigma(X_i)/\sigma(HNO_3{}^{IASI}) \times 100]$ with X_i referring to each of the i explanatory variables X, and expressed in %. Note that, although the distributions of the contribution of each proxy are not shown as a Figure, the calculated percentage values are used in the following discussion (next 3 subsections) to quantify the influence of the fitted parameters.

The annual cycle

The annual cycle, represented by the terms a_1 and b_1, shows large regression coefficients (Figure 11) and holds the largest part of the variability globally (up to 70% in the northern and southern mid to high latitudes), as was previously evidenced in Figure 8 (top panel). While the Brewer-Dobson circulation, which is embedded in these harmonic terms, influences to some extent the HNO_3 variability (through its influence on the conversion of N_2O to NO_y in the tropics and through the transport of NO_y-rich air masses towards the polar regions and subsequent transformation into HNO_3), the influence of the seasonality of the solar insolation is also likely to largely influence the annual seasonality, especially in the mid- to high latitudes. The increasing columns recorded during the winter in both polar regions can be explained by the combination of three processes: first, at low temperatures, HNO_3 is formed by heterogeneous reactions between N_2O_5 and $H_2O_{aerosol}$ and between $ClONO_2$ and $H_2O_{aerosol}$ or $HCl_{aerosol}$, which add to the main source gas-phase reaction $OH+NO_2+M \rightarrow HNO_3$. Second, while the source reactions of HNO_3 are still active, the loss reactions (HNO_3 photolysis and its reaction with OH) are significantly slowed down during the winter (Austin et al., 1986; McDonald et al., 2000; Santee et al., 2004). And third, as is mentioned is Section 3, with the decrease of the temperatures in the polar stratosphere, the winds inside the polar vortex gain intensity and induce a strong diabatic downward motion of air with little latitudinal mixing across the vortex boundary. This descending air from the upper stratosphere enriches the lower stratosphere in HNO_3 (Schoeberl and Hartmann, 1991; Manney et al., 1994; Santee et al., 1999).

The solar cycle, MEI, AO/AAO and QBO

The solar flux~~(SF)~~, ENSO index ~~(MEI)~~ and Arctic and Antarctic Oscillation (~~AO and AAO, respectively,~~ Figure 11) all have a similar influence in terms of magnitude (between -2.5×10^{15} and 2.5×10^{15} molec.cm^{-2}), although with different spatial patterns. The influence of the solar flux is positive in the northern polar latitudes and at the edge of eastern Antarctica, as well as above the Indian Ocean and Australia. It is close to zero or negative elsewhere. Previous studies showed that ozone changes due to the solar cycle are largest in the low stratosphere (Hood, 1997; Soukharev and Hood, 2006), which corresponds to the altitude of maximum sensitivity for HNO_3. Our results for the mid to high latitudes suggest opposite behaviour for HNO_3 (as was also reported for O_3 by Wespes et al. (2017)). However, the positive contribution of the solar cycle on the HNO_3 variation in the tropical stratosphere is in line with the low-latitude O_3 response previously reported (Soukharev and Hood, 2006; McCormack et al., 2007; Frossard et al., 2013; Maycock et al., 2016). Note also that the strong negative signal observed above western Antarctica is most probably due to the drawback of using for all seasons a constant emissivity for ocean surfaces (e.g. even when the ocean becomes frozen). For this reason, the regression coefficients in this area will not be discussed further.

The MEI shows a negative signal above the northern polar regions and in the eastern parts of the Pacific and Atlantic (especially ~~south of~~ west of South Africa) Oceans. A ~~weak~~ positive signal is observed above Australia and above the southern polar regions. Overall, the MEI influence is quite small, which is not surprising considering that it affects mostly the tropospheric circulation, where IASI is less sensitive. Its signature is nonetheless visible and significant in the eastern Pacific, where it contributes to up

to 30% of the HNO_3 variability, and in the mid-latitudes of the northern hemisphere~~, similarly to what was reported for~~ . The east-west gradient is in good agreement with chemical and dynamical effects of El Niño on O_3, and with previous studies that showed the same patterns for the influence of the MEI on O_3 ~~(Rieder et al., 2013)~~(Hood et al., 2010; Rieder et al., 2013; Wespes et al., 2017

The arctic oscillation (AO) signal is stronger, especially above the Atlantic Ocean, with a positive signal above eastern Canada and ~~Groenland~~ Greenland and between the north of eastern Africa and Florida. Except for those two regions, the ~~MEI~~ AO contributes at mid to high latitudes of the northern hemisphere with a negative signal, which contributes for $10-20\%$ to the HNO_3 variability. The corresponding proxy for the southern hemisphere (AAO) is also significant, with a strong positive signal above the vortex rim and a negative signal above Antarctica. These results are in agreement with previous studies that showed that, for O_3, both the arctic and antarctic oscillations (also called "annular modes") are ~~the~~ leading modes of variation in the extratropical atmosphere ~~. They largely~~ (Weiss et al., 2001; Frossard et al., 2013; de Laat et al., 2015; Wespes et al., 2017). They strongly influence the circulation up to the lower stratosphere and represent, particularly in the southern hemisphere, the fluctuations in the strength of the polar vortex ~~(Thompson and Wallace, 2000; Jones and Widmann, 2004; van den Broeke and van Lipzig, 2004; Wespes e~~

This further shows the ~~strong correlation~~ similarity in the behaviour of O_3 and HNO_3.

The QBO has a generally small influence on the distributions with, however, some contribution (up to 30%) in the equatorial band as expected (Baldwin et al., 2001; Solomon et al., 2014). As previously mentioned, several tests have been performed (not shown here) with the QBO taken at other pressure levels in the atmosphere (namely 20 and 50 hPa), and similar results have been obtained. Even though the QBO is a tropical phenomenon, its effects extend as far as the polar latitudes, through the modulation of the planetary Rossby waves (e.g. Holton and Tan (1980); Baldwin et al. (2001)). Because there are more topographical features in the northern hemisphere than in the southern hemisphere, these waves have a larger amplitude and can influence the polar stratospheric temperatures and hence the vortex formation. While the exact mechanism for the extratropical influence of the QBO is not exactly understood (Garfinkel et al., 2012; Solomon et al., 2014), it seems the large positive and negative signals observed in the northern high latitudes in Figure 11 can indeed be attributed to this modulation of the Rossby waves by the oscillation in the meridional circulation. This was also observed for O_3 by e.g. Wespes et al. (2017).

VPSC

The annual cycle, which is the dominant factor for HNO_3 variability at all latitudes, leading to the build-up of concentrations during the winter, is interrupted in the southern polar regions, particularly in the 70-90 S eqlat band (see also Figure 8), by the condensation and ~~further sedimenation~~ subsequent sedimentation of PSCs. The VPSC proxy, reflecting the volume of air below T_{NAT}, has a strong anti-correlated effect on HNO_3 columns, which decrease (negative values) with increasing VPSC ~~(Wang and Michelangeli, 2006; Lowe and MacKenzie, 2008; Kirner et al., 2015).~~(e.g. Wang and Michelangeli (2006); Lowe and MacKen

The signal of the VPSC proxy is thus, as expected, negative everywhere (in the polar regions considered), with values around -6×10^{15} molec.cm^{-2}. When looking at their contribution, we find that the ~~VPSC~~ PSCs account for a larger part of the HNO_3 variability ($40-60\%$) in the southern hemisphere, where the influence of denitrification is indeed expected to be more important, compared to the northern hemisphere (maxima of 40%), as discussed in Section 3 with the analysis of Figure 2. The small areas with a positive signal appear to be non significant (see grey crosses).

5 Conclusions

Time series of HNO_3 total columns retrieved from IASI/Metop between 2008 and 2016 have been presented and analyzed in terms of seasonal cycle and global variability. The analysis was conducted in terms of equivalent latitudes (here calculated on the basis of potential vorticity) and focused mainly on high latitude regions. We have shown that the IASI instrument captures the broad patterns of the seasonal cycles at all latitudes but also year-to-year specific behaviours. The systematic denitrification process occurring every winter-spring in the southern hemisphere shows up unambiguously in the time evolutions and the use of equivalent latitudes has enabled to isolate the regions affected based on the dominating stratospheric dynamical regimes. Three distinct zones within the polar regions were in particular separated; 1) the inner polar region (70-90 S), where the denitrification starts the earliest and where the HNO_3 columns reach their lowest values for the longest period; 2) the outer part of the polar vortex (65-70 S), where the HNO_3 columns drop occurs 1 month later and the minimum concentrations do not reach such low levels; 3) the polar vortex edges (55-65 S), where the columns follow a more normal annual cycle, with maxima around July, forming a collar of high columns around the denitrified vortex. The IASI-derived HNO_3 distributions also ~~reveal the unusual~~ reflect the denitrification periods in the northern hemisphere, during the exceptionally cold winters of 2011, 2014 and 2016.

The HNO_3 time series have been successfully fitted with multivariate regressions in order to identify the various factors responsible for the variability in the observations. To the best of our knowledge, this is the first time that such regression models are applied to the HNO_3 time evolution. A specific set of explanatory variables was retained for each equivalent latitude band following an iterative procedure, according to the influence of each of these variables in the regression. The regression model allowed good representation of the IASI observations in most cases (correlation coefficients between 0.81 and 0.94). However, the variability recorded ~~between~~ in the tropics could not be reproduced that well, with only about 20 to 40 % correctly accounted for. The regression for other parts of the globe yielded better results, especially in the southern polar regions, where a high percentage (60-80 %) of the observed variability is reproduced by the regression. Generally, it was found that the annual cycle is the factor responsible for the largest part of the variability, showing a hemispheric pattern. The Brewer-Dobson circulation, and also the solar insolation seasonality, which are embedded in the harmonic terms, seem to be the main drivers of variability, with the Brewer-Dobson circulation carrying NO_y towards the poles and both processes bringing the HNO_3 concentrations to their maxima during the local winter when production is enhanced and destruction inhibited~~(Mohanakumar, 2008; Butchart, 2014; Konopka et al., 2015)~~. We show interestingly that the polar stratospheric clouds contribute as the second most important driver of the variability of HNO_3 in the southern polar latitudes (65-90 S). The influence of PSCs is as expected less marked in the northern hemisphere, but ~~still allow improving significantly~~ accounting for PSCs still significantly improves the model-to-observation agreement especially during the colder northern winters (R from 0.83 to 0.86). While we feel that the VPSC proxy used here for the PSCs (including only the NAT) is generally good, it is not excluded that adding other forms of PSCs would further improve the model. In any case, the present work shows the potential of using the IASI measurements to study in depth the polar denitrification processes.

Going towards to the mid- and tropical latitudes, the annual cycle is still prominent, but the relative influence of the QBO

increases. Most of the weak seasonality revealed by IASI in the tropical regions is explained by the annual cycle (as well as a potential contribution of African fires and of lightning for additional NO_x sources), the QBO and the MEI.

More generally, this study shows that the IASI data allow a good analysis and understanding of the HNO_3 variability in the atmosphere. The measurements are made with exceptional spatial and temporal sampling, which allows a detailed analysis of the polar regions throughout the entire year. The amount of data allows ~~isolating statistically relevant features in the~~ for a thorough monitoring of the processes regulating the HNO_3 variability, such as the denitrification processes in the southern polar regions, or the seasonal variability in the tropical regions. The IASI HNO_3 time series will soon be extended with the launch of Metop C in September 2018, which should further improve the regression model. As shown here by the still significant residuals at some periods and locations, other factors could also probably be included to acquire a full and coherent representation of the HNO_3 total columns variability.

Acknowledgements. IASI has been developed and built under the responsibility of the "Centre National d'Etudes Spatiales" (CNES, France). It is flown on board the Metop satellites as part of the EUMETSAT Polar System. The IASI L1 data are received through the EUMETCast near-real-time data distribution service. The research was funded by the F.R.S.-FNRS, the Belgian State Federal Office for Scientific, Technical and Cultural Affairs (Prodex arrangement 4000111403 IASI.FLOW) and EUMETSAT through the Satellite Application Facility on ~~Ozone and atmospheric Chemistry Monitoring (O3MSAF~~Atmospheric Composition Monitoring (ACSAF). The authors would like to thank Ingo Wohltmann for the VPSC proxy and for useful discussions. G. Ronsmans is grateful to the "Fonds pour la Formation à la Recherche dans l'Industrie et dans l'Agriculture" of Belgium for a PhD grant (Boursier FRIA). Cathy Clerbaux is grateful to CNES for financial support.

References

Austin, J., Garcia, R. R., Russell, J. M., Solomon, S., and Tuck, A. F.: On the Atmospheric Photochemistry of Nitric Acid, Journal of Geophysical Research, 91, 5477–5485, https://doi.org/10.1029/JD091iD05p05477, 1986.

Austin, J., Hood, L. L., and Soukharev, B. E.: Solar cycle variations of stratospheric ozone and temperature in simulations of a coupled chemistry-climate model, Atmospheric Chemistry and Physics, 7, 1693–1706, https://doi.org/10.5194/acp-7-1693-2007, 2007.

Baldwin, M. P., Gray, L. J., Dunkerton, T. J., Hamilton, K., Haynes, P. H., Holton, J. R., Alexander, M. J., Hirota, I., Horinouchi, T., Jones, D. B. A., Marquardt, C., Sato, K., and Takahashi, M.: The quasi-biennial oscillation, Reviews of Geophysics, 39, 179–229, http://dx.doi.org/10.1029/1999RG000073, 2001.

Barbosa, P. M., Stroppiana, D., Grégoire, J., and Pereira, J. M. C.: An assessment of vegetation fire in Africa (1981-1991): Burned areas, burned biomass, and atmospheric emissions, Global Biogeochemical Cycles, 13, 933–950, https://doi.org/10.1029/1999GB900042, 1999.

Butchart, N.: The Brewer-Dobson circulation, Rev. Geophys, 52, 157–184, https://doi.org/10.1002/2013RG000448, 2014.

Chehade, W., Weber, M., and Burrows, J. P.: Total ozone trends and variability during 1979–2012 from merged data sets of various satellites, Atmospheric Chemistry and Physics, 14, 7059–7074, https://doi.org/10.5194/acp-14-7059-2014, 2014.

Clerbaux, C., Boynard, A., Clarisse, L., George, M., Hadji-Lazaro, J., Herbin, H., Hurtmans, D., Pommier, M., Razavi, A., Turquety, S., Wespes, C., and Coheur, P.-F.: Monitoring of atmospheric composition using the thermal infrared IASI/MetOp sounder, Atmospheric Chemistry and Physics, 9, 6041–6054, https://doi.org/10.5194/acp-9-6041-2009, 2009.

Cooper, M., Martin, R. V., Wespes, C., Coheur, P.-F., Clerbaux, C., and Murray, L. T.: Tropospheric nitric acid columns from the IASI satellite instrument interpreted with a chemical transport model: Implications for parametrizations of nitric oxide production by lightning, Journal of Geophysical Research, 119, 68–79, https://doi.org/10.1002/2014JD021907, 2014.

Covington, A. E.: Solar Noise Observations on 10.7 Centimeters, Proceedings of the IRE, 36, 454–457, https://doi.org/10.1109/JRPROC.1948.234598, 1948.

de Laat, A. T. J. and van Weele, M.: The 2010 Antarctic ozone hole: Observed reduction in ozone destruction by minor sudden stratospheric warmings, Scientific Reports, 1, 38, https://doi.org/10.1038/srep00038, 2011.

de Laat, A. T. J., van der A, R. J., and van Weele, M.: Tracing the second stage of ozone recovery in the Antarctic ozone-hole with a "big data" approach to multivariate regressions, Atmospheric Chemistry and Physics, 15, 79–97, https://doi.org/10.5194/acp-15-79-2015, 2015.

Drdla, K. and Müller, R.: Temperature thresholds for polar stratospheric ozone loss, Atmospheric Chemistry and Physics Discussions, 10, 28 687–28 720, https://doi.org/10.5194/acpd-10-28687-2010, 2010.

Finlayson-Pitts, B. J. and Pitts, J. N.: Chemistry of the Upper and Lower Atmosphere, Elsevier, https://doi.org/https://doi.org/10.1016/B978-012257060-5/50025-3, 2000.

Fischer, H., Waibel, A. E., Welling, M., Wienhold, F. G., Zenker, T., Crutzen, P. J., Arnold, F., Bürger, V., Schneider, J., Bregman, A., Lelieveld, J., and Siegmund, P. C.: Observations of high concentration of total reactive nitrogen (NOy) and nitric acid (HNO3) in the lower Arctic stratosphere during the Stratosphere-Troposphere Experiment by Aircraft Measurements (STREAM) II campaign in February 1995, Journal of Geophysical Research, 102, 23 559, https://doi.org/10.1029/97JD02012, 1997.

Frossard, L., Rieder, H. E., Ribatet, M., Staehelin, J., Maeder, J. A., Di Rocco, S., Davison, A. C., and Peter, T.: On the relationship between total ozone and atmospheric dynamics and chemistry at mid-latitudes – Part 1: Statistical models and spatial fingerprints of atmospheric dynamics and chemistry, Atmospheric Chemistry and Physics Discussions, 12, 13 161–13 199, https://doi.org/10.5194/acp-13-147-2013, 2013.

Garfinkel, C. I., Shaw, T. A., Hartmann, D. L., and Waugh, D. W.: Does the Holton–Tan Mechanism Explain How the Quasi-Biennial Oscillation Modulates the Arctic Polar Vortex?, Journal of the Atmospheric Sciences, 69, 1713–1733, https://doi.org/10.1175/JAS-D-11-0209.1, 2012.

Garfinkel, C. I., Hurwitz, M. M., and Oman, L. D.: Effect of recent sea surface temperature trends on the Arctic stratospheric vortex, Journal of Geophysical Research Atmospheres, 120, 5404–5416, https://doi.org/10.1002/2015JD023284, 2015.

Gobbi, G. P., Deshler, T., Adriani, A., and Hofmann, D. J.: Evidence for denitrification in the 1990 Antarctic spring stratosphere: I, Lidar and temperature measurements, Geophysical Research Letters, 18, 1995–1998, https://doi.org/10.1029/91GL02310, 1991.

Gong, D. and Wang, S.: Definition of Antarctic Oscillation index, Geophysical Research Letters, 26, 459–462, https://doi.org/10.1029/1999GL900003, 1999.

Hanson, D. and Mauersberger, K.: Laboratory studies of the nitric acid trihydrate: Implications for the south polar stratosphere, Geophysical Research Letters, 15, 855–858, https://doi.org/10.1029/GL015i008p00855, 1988.

Harris, N. R. P., Lehmann, R., Rex, M., and von der Gathen, P.: A closer look at Arctic ozone loss and polar stratospheric clouds, Atmospheric Chemistry and Physics, 10, 8499–8510, https://doi.org/10.5194/acp-10-8499-2010, 2010.

Hauchecorne, A., Bertaux, J. L., Dalaudier, F., Keckhut, P., Lemennais, P., Bekki, S., Marchand, M., Lebrun, J. C., Kyrölä, E., Tamminen, J., Sofieva, V., Fussen, D., Vanhellemont, F., Fanton Dandon, O., Barrot, G., Blanot, L., Fehr, T., and Saavedra De Miguel, L.: Response of tropical stratospheric O3, NO2 and NO3 to the equatorial Quasi-Biennial Oscillation and to temperature as seen from GOMOS/ENVISAT, Atmospheric Chemistry and Physics, 10, 8873–8879, https://doi.org/10.5194/acp-10-8873-2010, 2010.

Hilton, F., Armante, R., August, T., Barnet, C., Bouchard, A., Camy-Peyret, C., Capelle, V., Clarisse, L., Clerbaux, C., Coheur, P.-F., Collard, A., Crevoisier, C., Dufour, G., Edwards, D., Faijan, F., Fourrié, N., Gambacorta, A., Goldberg, M., Guidard, V., Hurtmans, D., Illingworth, S., Jacquinet-Husson, N., Kerzenmacher, T., Klaes, D., Lavanant, L., Masiello, G., Matricardi, M., McNally, A., Newman, S., Pavelin, E., Payan, S., Péquignot, E., Peyridieu, S., Phulpin, T., Remedios, J., Schlüssel, P., Serio, C., Strow, L., Stubenrauch, C., Taylor, J., Tobin, D., Wolf, W., and Zhou, D.: Hyperspectral Earth Observation from IASI: Five Years of Accomplishments, Bulletin of the American Meteorological Society, 93, 347–370, https://doi.org/10.1175/BAMS-D-11-00027.1, 2012.

Holton, J. R. and Tan, H.-C.: The Influence of the Equatorial Quasi-Biennial Oscillation on the Global Circulation at 50 mb, https://doi.org/10.1175/1520-0469(1980)037<2200:TIOTEQ>2.0.CO;2, 1980.

Hood, L. L.: The solar cycle variation of total ozone: Dynamical forcing in the lower stratosphere, J. Geophys. Res., 102, 1355–1370, https://doi.org/10.1029/2007JD009391, 1997.

Hood, L. L. and Soukharev, B. E.: Quasi-Decadal Variability of the Tropical Lower Stratosphere: The Role of Extratropical Wave Forcing, Journal of the Atmospheric Sciences, 60, 2389–2403, https://doi.org/10.1175/1520-0469(2003)060<2389:QVOTTL>2.0.CO;2, 2003.

Hood, L. L., Soukharev, B. E., and McCormack, J. P.: Decadal variability of the tropical stratosphere: Secondary influence of the El NiñoSouthern Oscillation, Journal of Geophysical Research Atmospheres, 115, 1–16, https://doi.org/10.1029/2009JD012291, 2010.

Hoyle, C. R., Engel, I., Luo, B. P., Pitts, M. C., Poole, L. R., Grooß, J. U., and Peter, T.: Heterogeneous formation of polar stratospheric clouds-Part 1: Nucleation of nitric acid trihydrate (NAT), Atmospheric Chemistry and Physics, 13, 9577–9595, https://doi.org/10.5194/acp-13-9577-2013, 2013.

Hurtmans, D., Coheur, P.-F., Wespes, C., Clarisse, L., Scharf, O., Clerbaux, C., Hadji-Lazaro, J., George, M., and Turquety, S.: FORLI radiative transfer and retrieval code for IASI, Journal of Quantitative Spectroscopy and Radiative Transfer, 113, 1391–1408, https://doi.org/10.1016/j.jqsrt.2012.02.036, 2012.

Jacob, D. J.: Heterogeneous chemistry and tropospheric ozone, Atmospheric Environment, 34, 2131–2159, https://doi.org/10.1016/S1352-2310(99)00462-8, 2000.

Jones, J. M. and Widmann, M.: Early peak in Antarctic oscillation index, Nature, 432, 290–291, https://doi.org/10.1038/432290b, 2004.

Khosrawi, F., Urban, J., Lossow, S., Stiller, G., Weigel, K., Braesicke, P., Pitts, M. C., Rozanov, A., Burrows, J. P., and Murtagh, D.: Sensitivity of polar stratospheric cloud formation to changes in water vapour and temperature, Atmospheric Chemistry and Physics, 16, 101–121, https://doi.org/10.5194/acp-16-101-2016, 2016.

Kirner, O., Ruhnke, R., Buchholz-Dietsch, J., Jöckel, P., Brühl, C., and Steil, B.: Simulation of polar stratospheric clouds in the chemistry-climate-model EMAC via the submodel PSC, Geoscientific Model Development, 4, 169–182, https://doi.org/10.5194/gmd-4-169-2011, 2011.

Kirner, O., Müller, R., Ruhnke, R., and Fischer, H.: Contribution of liquid, NAT and ice particles to chlorine activation and ozone depletion during Antarctic winter and spring, Atmospheric Chemistry and Physics, 15, 2019–2030, https://doi.org/10.5194/acp-15-2019-2015, 2015.

Klekociuk, A., Tully, M., Alexander, S., Dargaville, R., Deschamps, L., Fraser, P., Gies, H., Henderson, S., Javorniczky, J., Krummel, P., Petelina, S., Shanklin, J., Siddaway, J., and Stone, K.: The Antarctic ozone hole during 2010, Australian Meteorological and Oceanographic Journal, 61, 253–267, https://doi.org/10.22499/2.6104.006, 2011.

Knibbe, J. S., van der A, R. J., and de Laat, A. T. J.: Spatial regression analysis on 32 years of total column ozone data, Atmospheric Chemistry and Physics, 14, 8461–8482, https://doi.org/10.5194/acp-14-8461-2014, 2014.

Kodera, K. and Kuroda, Y.: Tropospheric and stratospheric aspects of the Arctic Oscillation, Geophysical Research Letters, 27, 3349–3352, https://doi.org/10.1029/2000GL012017, 2000.

Kodera, K. and Kuroda, Y.: Dynamical response to the solar cycle, Journal of Geophysical Research Atmospheres, 107, 1–12, https://doi.org/10.1029/2002JD002224, 2002.

Konopka, P., Ploeger, F., Tao, M., Birner, T., and Riese, M.: Hemispheric asymmetries and seasonality of mean age of air in the lower stratosphere: Deep versus shallow branch of the Brewer-Dobson circulation, Journal of Geophysical Research: Atmospheres, 120, https://doi.org/10.1002/2014JD022429.Received, 2015.

Kyrölä, E., Tamminen, J., Sofieva, V., Bertaux, J. L., Hauchecorne, A., Dalaudier, F., Fussen, D., Vanhellemont, F., Fanton D'Andon, O., Barrot, G., Guirlet, M., Fehr, T., and Saavedra De Miguel, L.: GOMOS O3, NO2, and NO3 observations in 2002-2008, Atmospheric Chemistry and Physics, 10, 7723–7738, https://doi.org/10.5194/acp-10-7723-2010, 2010.

Labrador, L. J., Von Kuhlmann, R., and Lawrence, M. G.: Strong sensitivity of the global mean OH concentration and the tropospheric oxidizing efficiency to the source of NOx from lightning, Geophysical Research Letters, 31, L06 102, https://doi.org/10.1029/2003GL019229, 2004.

Lambert, A., Santee, M. L., and Livesey, N. J.: Interannual variations of early winter Antarctic polar stratospheric cloud formation and nitric acid observed by CALIOP and MLS, Atmospheric Chemistry and Physics, 16, 15 219–15 246, https://doi.org/10.5194/acp-16-15219-2016, 2016.

Lary, D. J.: Catalytic destruction of stratospheric ozone, Journal of Geophysical Research, 102, 21 515–21 526, https://doi.org/10.1029/97JD00912, 1997.

Lee, A. M., Roscoe, H. K., Jones, A. E., Haynes, P. H., Shuckburgh, E. F., Morrey, M. W., and Pumphrey, H. C.: The impact of the mixing properties within the Antarctic stratospheric vortex on ozone loss in spring, Journal of Geophysical Research, 106, 3203–3211, https://doi.org/10.1029/2000JD900398, 2001.

Lee, H. and Smith, A. K.: Simulation of the combined effects of solar cycle, quasi-biennial oscillation, and volcanic forcing on stratospheric ozone changes in recent decades, Journal of Geophysical Research, 108, 1–16, https://doi.org/10.1029/2001JD001503, 2003.

Lee, S., Shelow, D. M., Thompson, A. M., and Miller, S. K.: QBO and ENSO variability in temperature and ozone from SHADOZ, 1998-2005, Journal of Geophysical Research Atmospheres, 115, 1998–2005, https://doi.org/10.1029/2009JD013320, 2010.

Lowe, D. and MacKenzie, A. R.: Polar stratospheric cloud microphysics and chemistry, Journal of Atmospheric and Solar-Terrestrial Physics, 70, 13–40, https://doi.org/10.1016/j.jastp.2007.09.011, 2008.

Mäder, J. A., Staehelin, J., Brunner, D., Stahel, W. A., Wohltmann, I., and Peter, T.: Statistical modeling of total ozone: Selection of appropriate explanatory variables, Journal of Geophysical Research, 112, https://doi.org/10.1029/2006JD007694, 2007.

Mäder, J. A., Staehelin, J., Peter, T., Brunner, D., Rieder, H. E., and Stahel, W. A.: Evidence for the effectiveness of the Montreal Protocol to protect the ozone layer, Atmospheric Chemistry and Physics, 10, 12 161–12 171, https://doi.org/10.5194/acp-10-12161-2010, 2010.

Manney, G. L. and Lawrence, Z. D.: The major stratospheric final warming in 2016: Dispersal of vortex air and termination of Arctic chemical ozone loss, Atmospheric Chemistry and Physics, 16, 15 371–15 396, https://doi.org/10.5194/acp-16-15371-2016, 2016.

Manney, G. L., Zurek, R., O'Neill, A., and Swinbank, R.: On the motion of air through the stratospheric polar vortex, Journal of the Atmospheric Sciences, 51, 2973–2994, https://doi.org/10.1175/1520-0469(1994)051<2973:OTMOAT>2.0.CO;2, 1994.

Manney, G. L., Michelsen, H. A., Santee, M. L., Gunson, M. R., Irion, F. W., Roche, A. E., and Livesey, N. J.: Polar vortex dynamics during spring and fall diagnosed using trace gas observations from the Atmospheric Trace Molecule Spectroscopy instrument, Journal of Geophysical Research: Atmospheres, 104, 18 841–18 866, https://doi.org/10.1029/1999JD900317, 1999.

Manney, G. L., Santee, M. L., Rex, M., Livesey, N. J., Pitts, M. C., Veefkind, P., Nash, E. R., Wohltmann, I., Lehmann, R., Froidevaux, L., Poole, L. R., Schoeberl, M. R., Haffner, D. P., Davies, J., Dorokhov, V., Gernandt, H., Johnson, B., Kivi, R., Kyrö, E., Larsen, N., Levelt, P. F., Makshtas, A., McElroy, C. T., Nakajima, H., Parrondo, M. C., Tarasick, D. W., von der Gathen, P., Walker, K. A., and Zinoviev, N. S.: Unprecedented Arctic ozone loss in 2011, Nature, 478, 469–475, https://doi.org/10.1038/nature10556, 2011.

Matthias, V., Dörnbrack, A., and Stober, G.: The extraordinarily strong and cold polar vortex in the early northern winter 2015/2016, Geophysical Research Letters, 43, 12,287–12,294, https://doi.org/10.1002/2016GL071676, 2016.

Maycock, A., Matthes, K., Tegtmeier, S., Thiéblemont, R., and Hood, L.: The representation of solar cycle signals in stratospheric ozone -Part 1: A comparison of satellite observations, Atmospheric Chemistry and Physics Discussions, pp. 1–52, https://doi.org/10.5194/acp-2015-882, http://www.atmos-chem-phys-discuss.net/acp-2015-882/, 2016.

McCormack, J. P., Siskind, D. E., and Hood, L. L.: Solar-QBO interaction and its impact on stratospheric ozone in a zonally averaged photochemical transport model of the middle atmosphere, Journal of Geophysical Research Atmospheres, 112, https://doi.org/10.1029/2006JD008369, 2007.

McDonald, M., de Zafra, R., and Muscari, G.: Millimeter wave spectroscopic measurements over the South Pole 5 . Morphology and evolution of HNO3 vertical distribution, 1993 versus 1995, Journal of Geophysical Research, 105, 17 739–17 750, https://doi.org/10.1029/2000JD900120, 2000.

Miller, A. J., Cai, A., Tiao, G., Wuebbles, D. J., Flynn, L. E., Yang, S. K., Weatherhead, E. C., Fioletov, V., Petropavlovskikh, I., Meng, X. L., Guillas, S., Nagatani, R. M., and Reinsel, G. C.: Examination of ozonesonde data for trends and trend changes incorporating solar and Arctic oscillation signals, Journal of Geophysical Research: Atmospheres, 111, 1–10, https://doi.org/10.1029/2005JD006684, 2006.

Mohanakumar, K.: Stratosphere Troposphere Interactions - An Introduction, https://doi.org/10.1007/978-1-4020-8217-7, 2008.

Morgenstern, O., Braesicke, P., Hurwitz, M. M., O'Connor, F. M., Bushell, A. C., Johnson, C. E., and Pyle, J. A.: The world avoided by the Montreal Protocol, Geophysical Research Letters, 35, 1–5, https://doi.org/10.1029/2008GL034590, 2008.

Neuman, J. A., Gao, R. S., Fahey, D. W., Holecek, J. C., Ridley, B. A., Walega, J. G., Grahek, F. E., Richard, E. C., McElroy, C. T., Thompson, T. L., Elkins, J. W., Moore, F. L., and Ray, E. A.: In situ measurements of HNO3 , NOy , NO , and O3 in the lower stratosphere and upper troposphere, Atmospheric Environment, 35, 5789–5797, https://doi.org/10.1016/S1352-2310(01)00354-5, 2001.

Newman, P. A., Nash, E. R., and Rosenfield, J. E.: What controls the temperature of the Arctic stratosphere during the spring?, Journal of Geophysical Research, 106, 19 999–20 010, https://doi.org/10.1029/2000jd000061, 2001.

Peter, T.: Microphysics and heterogeneous chemistry of polar stratospheric clouds, Annual Review of Physical Chemistry, 48, 785–822, https://doi.org/10.1146/annurev.physchem.48.1.785, 1997.

Piccolo, C. and Dudhia, A.: Precision validation of MIPAS-Envisat products, Atmospheric Chemistry and Physics, 7, 1915–1923, https://doi.org/10.5194/acp-7-1915-2007, 2007.

Pitts, M. C., Poole, L. R., and Thomason, L. W.: CALIPSO polar stratospheric cloud observations: second-generation detection algorithm and composition discrimination, Atmospheric Chemistry and Physics, 9, 7577–7589, https://doi.org/10.5194/acp-9-7577-2009, 2009.

Popp, P. J., Marcy, T. P., Gao, R. S., Watts, L. A., Fahey, D. W., Richard, E. C., Oltmans, S. J., Santee, M. L., Livesey, N. J., Froidevaux, L., Sen, B., Toon, G. C., Walker, K. A., Boone, C. D., and Bernath, P. F.: Stratospheric correlation between nitric acid and ozone, Journal of Geophysical Research, 114, D03 305, https://doi.org/10.1029/2008JD010875, 2009.

Randel, W. J. and Thompson, A. M.: Interannual variability and trends in tropical ozone derived from SAGE II satellite data and SHADOZ ozonesondes, Journal of Geophysical Research Atmospheres, 116, 1–9, https://doi.org/10.1029/2010JD015195, 2011.

Randel, W. J., Garcia, R. R., Calvo, N., and Marsh, D.: ENSO influence on zonal mean temperature and ozone in the tropical lower stratosphere, Geophysical Research Letters, 36, 1–5, https://doi.org/10.1029/2009GL039343, 2009.

Rieder, H. E., Frossard, L., Ribatet, M., Staehelin, J., Maeder, J. A., Di Rocco, S., Davison, A. C., Peter, T., Weihs, P., and Holawe, F.: On the relationship between total ozone and atmospheric dynamics and chemistry at mid-latitudes – Part 2: The effects of the El Niño/Southern Oscillation, volcanic eruptions and contributions of atmospheric dynamics and chemistry to long-term total ozone, Atmospheric Chemistry and Physics, 12, 13 201–13 236, https://doi.org/https://doi.org/10.5194/acp-13-165-2013, 2013.

Rodgers, C. D.: Inverse Methods for Atmospheric Sounding - Theory and Practice, vol. 2 of *Series on Atmospheric Oceanic and Planetary Physics*, World Scientific Publishing Co. Pte. Ltd., https://doi.org/10.1142/9789812813718, 2000.

Ronsmans, G., Langerock, B., Wespes, C., Hannigan, J. W., Hase, F., Kerzenmacher, T., Mahieu, E., Schneider, M., Smale, D., Hurtmans, D., De Mazière, M., Clerbaux, C., and Coheur, P.-F.: First characterization and validation of FORLI-HNO3 vertical profiles retrieved from IASI/Metop, Atmospheric Measurement Techniques, 9, 4783–4801, https://doi.org/10.5194/amt-9-4783-2016, 2016.

Roscoe, H. K., Feng, W., Chipperfield, M. P., Trainic, M., and Shuckburgh, E. F.: The existence of the edge region of the Antarctic stratospheric vortex, Journal of Geophysical Research Atmospheres, 117, 1–12, https://doi.org/10.1029/2011JD015940, 2012.

Santee, M. L., Manney, G. L., Froidevaux, L., Read, W. G., and Waters, J. W.: Six years of UARS Microwave Limb Sounder HNO3 observations : Seasonal, interhemispheric, and interannual variations in the lower stratosphere, Journal of Geophysical Research, 104, 8225–8246, https://doi.org/10.1029/1998JD100089, 1999.

Santee, M. L., Manney, G. L., Livesey, N. J., and Read, W. G.: Three-dimensional structure and evolution of stratospheric HNO3 based on UARS microwave limb sounder measurements, Journal of Geophysical Research D: Atmospheres, 109, 1–19, https://doi.org/10.1029/2004JD004578, 2004.

Santee, M. L., Manney, G. L., Livesey, N. J., Froidevaux, L., MacKenzie, I. A., Pumphrey, H. C., Read, W. G., Schwartz, M. J., Waters, J. W., and Harwood, R. S.: Polar processing and development of the 2004 Antarctic ozone hole: First results from MLS on Aura, Geophysical Research Letters, 32, 1–4, https://doi.org/10.1029/2005GL022582, 2005.

Sauvage, B., Martin, R. V., van Donkelaar, A., and Ziemke, J. R.: Quantification of the factors controlling tropical tropospheric ozone and the South Atlantic maximum, Journal of Geophysical Research Atmospheres, 112, 1–14, https://doi.org/10.1029/2006JD008008, 2007.

Schirber, S.: Influence of ENSO on the QBO: Results from an ensemble of idealized simulations, Journal of Geophysical Research: Atmospheres, 120, 1109–1122, https://doi.org/10.1002/2014JD022460, 2015.

Schoeberl, M. R. and Hartmann, D. L.: The Dynamics of the Stratospheric Polar Vortex and Its Relation to Springtime Ozone Depletions, Science, 251, 46–52, https://doi.org/10.1126/science.251.4989.46, 1991.

Scholes, R., Ward, D., and Justice, C.: Emissions of trace gases and aerosol particles due to vegetation burning in southern hemisphere Africa, Journal of Geophysical Research, 101, 23 677–23 682, https://doi.org/10.1029/95JD02049, 1996.

Schreier, S. F., Richter, A., Kaiser, J. W., and Burrows, J. P.: The empirical relationship between satellite-derived tropospheric NO2 and fire radiative power and possible implications for fire emission rates of NOx, Atmospheric Chemistry and Physics, 14, 2447–2466, https://doi.org/10.5194/acp-14-2447-2014, 2014.

Sioris, C. E., McLinden, C. A., Fioletov, V. E., Adams, C., Zawodny, J. M., Bourassa, A. E., Roth, C. Z., and Degenstein, D. A.: Trend and variability in ozone in the tropical lower stratosphere over 2.5 solar cycles observed by SAGE II and OSIRIS, Atmospheric Chemistry and Physics, 14, 3479–3496, https://doi.org/10.5194/acp-14-3479-2014, 2014.

Solomon, A., Richter, J. H., and Bacmeister, J. T.: An objective analysis of the QBO in ERA-Interim and the Community Atmosphere Model, version 5, Geophysical Research Letters, 41, 7791–7798, https://doi.org/10.1002/2014GL061801, 2014.

Solomon, S.: Stratospheric ozone depletion: A review of concepts and history, Reviews of Geophysics, 37, 275–316, https://doi.org/10.1029/1999RG900008, 1999.

Soukharev, B. E. and Hood, L. L.: Solar cycle variation of stratospheric ozone: Multiple regression analysis of long-term satellite data sets and comparisons with models, Journal of Geophysical Research: Atmospheres, 111, 1–18, https://doi.org/10.1029/2006JD007107, 2006.

Steinbrecht, W.: Enhanced upper stratospheric ozone: Sign of recovery or solar cycle effect?, Journal of Geophysical Research, 109, 1–6, https://doi.org/10.1029/2003JD004284, 2004.

Tabazadeh, A., Toon, O. B., and Jensen, E. J.: Formation and implications of ice particle nucleation in the stratosphere, Geophysical Research Letters, 24, 2007–2010, https://doi.org/10.1029/97GL01883, 1997.

Tapping, K. F.: The 10.7 cm solar radio flux (F10.7), Space Weather, 11, 394–406, https://doi.org/10.1002/swe.20064, 2013.

Tapping, K. F. and DeTracey, B.: The origin of the 10.7 cm flux, Solar Physics, 127, 321–332, https://doi.org/10.1007/BF00152171, 1990.

Thompson, D. W. J. and Wallace, J. M.: Annular Modes in the Extratropical Circulation. Part I : Month-to-Month Variability, Journal of Climate, 13, 1000–1016, https://doi.org/10.1175/1520-0442(2000)01360;1000:amitec62;2.0.co;2, 2000.

Toon, G. C., Farmer, C. B., Lowes, L. L., Schaper, P. W., Blavier, J., and Norton, R. H.: Infrared Aircraft Measurements of Stratospheric Composition Over Antarctica During September 1987, Journal of Geophysical Research, 94, 16 571–16 596, https://doi.org/10.1029/JD094iD14p16571, 1989.

Trenberth, K. E., Branstator, G. W., Karoly, D., Kumar, A., Lau, N.-C., and Ropelewski, C.: Progress during TOGA in understanding and modeling global teleconnections associated with tropical sea surface temperatures, Journal of Geophysical Research: Oceans, 103, 14 291–14 324, https://doi.org/10.1029/97JC01444, 1998.

Urban, J., Pommier, M., Murtagh, D. P., Santee, M. L., and Orsolini, Y. J.: Nitric acid in the stratosphere based on Odin observations from 2001 to 2009 – Part 1 : A global climatology, Atmospheric Chemistry and Physics, 9, 7031–7044, https://doi.org/10.5194/acp-9-7031-2009, 2009.

Valks, P., Pinardi, G., Richter, A., Lambert, J. C., Hao, N., Loyola, D., Van Roozendael, M., and Emmadi, S.: Operational total and tropospheric NO2 column retrieval for GOME-2, Atmospheric Measurement Techniques, 4, 1491–1514, https://doi.org/10.5194/amt-4-1491-2011, 2011.

Van Damme, M., Whitburn, S., Clarisse, L., Clerbaux, C., Hurtmans, D., and Coheur, P.-F.: Version 2 of the IASI NH3 neural network retrieval algorithm: near-real time and reanalysed datasets, Atmospheric Measurement Techniques, 10, 4905–4914, https://doi.org/10.5194/amt-2017-239, 2017.

van den Broeke, M. R. and van Lipzig, N. P. M.: Changes in Antarctic temperature, wind and precipitation in response to the Antarctic Oscillation, Annals of Glaciology, 39, 119–126, https://doi.org/10.3189/172756404781814654, 2004.

Voigt, C., Schreiner, J., Kohlmann, A., Zink, P., Mauersberger, K., Larsen, N., Deshler, T., Kro, C., Rosen, J., Adriani, A., Cairo, F., Donfrancesco, G. D., Viterbini, M., Ovarlez, J., Ovarlez, H., and David, C.: Nitric Acid Trihydrate (NAT) in Polar Stratospheric Clouds, Science, 290, 1756–1758, https://doi.org/10.1126/science.290.5497.1756, 2000.

von König, M., Bremer, H., Kleinböhl, A., Küllmann, H., Künzi, K. F., Goede, A. P. H., Browell, E. V., Grant, W. B., Burris, J. F., McGee, T. J., and Twigg, L.: Using gas-phase nitric acid as an indicator of PSC composition, Journal of Geophysical Research, 107, SOL 8–1–SOL 8–10, https://doi.org/10.1029/2001JD001041, 2002.

Wang, D. Y., Blom, C. E., Ward, W. E., Fischer, H., Blumenstock, T., Hase, F., Keim, C., Liu, G. Y., Mikuteit, S., Oelhaf, H., Wetzel, G., Cortesi, U., Mencaraglia, F., Bianchini, G., Redaelli, G., Pirre, M., Catoire, V., Huret, N., Vigouroux, C., Mahieu, E., Demoulin, P., Wood, S., Smale, D., Jones, N., Nakajima, H., Sugita, T., Urban, J., Murtagh, D., Boone, C. D., Bernath, P. F., Walker, K. a., Kuttippurath, J., Toon, G., Piccolo, C., Brunswick, N., Zealand, N., Science, S., and Cedex, P.: Validation of MIPAS HNO3 operational data, Atmospheric Chemistry and Physics, 7, 4905–4934, https://doi.org/10.5194/acp-7-4905-2007, 2007.

Wang, X. and Michelangeli, D. V.: A review of polar stratospheric cloud formation, China Particuology, 4, 261–271, https://doi.org/10.1016/S1672-2515(07)60275-9, 2006.

Wegner, T., Grooß, J.-U., von Hobe, M., Stroh, F., Sumińska-Ebersoldt, O., Volk, C. M., Hösen, E., Mitev, V., Shur, G., and Müller, R.: Heterogeneous chlorine activation on stratospheric aerosols and clouds in the Arctic polar vortex, Atmospheric Chemistry and Physics, 12, 11 095–11 106, https://doi.org/10.5194/acp-12-11095-2012, 2012.

Weiss, A. K., Staehelin, J., Appenzeller, C., and Harris, N. R. P.: Chemical and dynamical contributions to ozone profile trends of the Payerne (Switzerland) balloon soundings, Journal of Geophysical Research: Atmospheres, 106, 22 685–22 694, https://doi.org/10.1029/2000JD000106, 2001.

Wespes, C., Hurtmans, D., Clerbaux, C., Santee, M. L., Martin, R. V., and Coheur, P. F.: Global distributions of nitric acid from IASI/MetOP measurements, Atmospheric Chemistry and Physics, 9, 8035–8069, https://doi.org/10.5194/acpd-9-8035-2009, 2009.

Wespes, C., Coheur, P.-F., Emmons, L. K., Hurtmans, D., Safieddine, S., Clerbaux, C., and Edwards, D. P.: Ozone variability in the troposphere and the stratosphere from the first six years of IASI observations (2008–2013), Atmospheric Chemistry and Physics Discussions, 15, 27 575–27 625, https://doi.org/10.5194/acpd-15-27575-2015, 2016.

Wespes, C., Hurtmans, D., Clerbaux, C., and Coheur, P.-F.: O3 variability in the troposphere as observed by IASI over 2008-2016: Contribution of atmospheric chemistry and dynamics, Journal of Geophysical Research: Atmospheres, 122, 2429–2451, https://doi.org/10.1002/2016JD025875, http://doi.wiley.com/10.1002/2016JD025875, 2017.

WMO: Scientific Assessment of Ozone Depletion: 2014, Global Ozone Research and Monitoring Project – Report No. 55, World Meteorological Organization, Geneva, Switzerland, 2014.

Wohltmann, I., Lehmann, R., Rex, M., Brunner, D., and Mäder, J. A.: A process-oriented regression model for column ozone, Journal of Geophysical Research, 112, 1–18, https://doi.org/10.1029/2006JD007573, 2007.

Wohltmann, I., Lehmann, R., and Rex, M.: Update of the Polar SWIFT model for polar stratospheric ozone loss (Polar SWIFT version 2), Geoscientific Model Development, 10, 2671–2689, https://doi.org/10.5194/gmd-10-2671-2017, 2017.

Wolter, K. and Timlin, M. S.: Monitoring ENSO in COADS with a seasonally adjusted principal component index, in: Proceedings of the 17th Climate Diagnostics Workshop, edited by NOAA/NMC/CAC, pp. 52–57, CNSSL, IMMS and the School of Meteor., Univ. of Oklahoma, Norman, OK, 1993.

Wolter, K. and Timlin, M. S.: Measuring the strength of ENSO events - how does 1997/98 rank?, Weather, 53, 315–324, https://doi.org/10.1002/j.1477-8696.1998.tb06408.x, 1998.

Table 1. Proxies used for the regressions and their source

Proxy	Description	Source
SF	Solar Flux at 10.7 cm	NOAA National Center for Environmental Information https://www.ngdc.noaa.gov/stp/solar/flux.html
QBO	Quasi Biennial Oscillation index at 10 and 30hPa	Free University of Berlin http://www.geo.fu-berlin.de/en/met/ag/strat/ produkte/qbo/index.html
MEI	Multivariate ENSO Index	NOAA Earth System Research Laboratory http://www.esrl.noaa.gov/psd/data/climateindices/
VPSC	Volume of Nitric Acid Trihydrates formed in the stratosphere	Dr. Ingo Wohltmann at AWI (personal communication)
AO & AAO	Arctic & Antarctic oscillation indices	NOAA Earth System Research Laboratory http://www.esrl.noaa.gov/psd/data/climateindices/

Table 2. Set of variables retained by the selection algorithm for each equivalent latitude band.

70-90S	65-70S	55-65S	40-55S	30-40S	30-30	30-40N	40-55N	55-65N	65-70N	70-90N
	SF	SF	SF	SF	SF	SF	SF	SF	SF	
QBO10	QBO10	QBO10	QBO10	QBO10	QBO10	QBO10	QBO10	QBO10	QBO10	QBO10
		QBO30	QBO30	QBO30	QBO30	QBO30	QBO30	QBO30	QBO30	QBO30
COS1	COS1	COS1	COS1	COS1	COS1	COS1	COS1	COS1	COS1	COS1
SIN1	SIN1	SIN1	SIN1	SIN1	SIN1	SIN1	SIN1	SIN1	SIN1	SIN1
MEI	MEI	MEI	MEI	MEI	MEI	MEI	MEI	MEI		
VPSC	VPSC								VPSC	VPSC
	AAO	AAO	AAO	AAO	AO/AAO	AO	AO	AO		AO

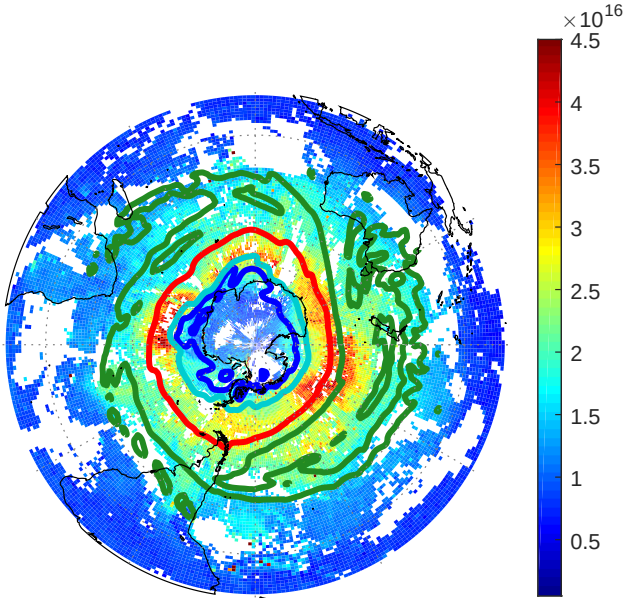

Figure 1. Example of equivalent latitude contours for -70 (blue), -65 (light blue), -55 (red) and -40 (green) equivalent latitudes. The background colors are HNO_3 total columns (daily mean for 21.07.2011, in molec.cm^{-2}).

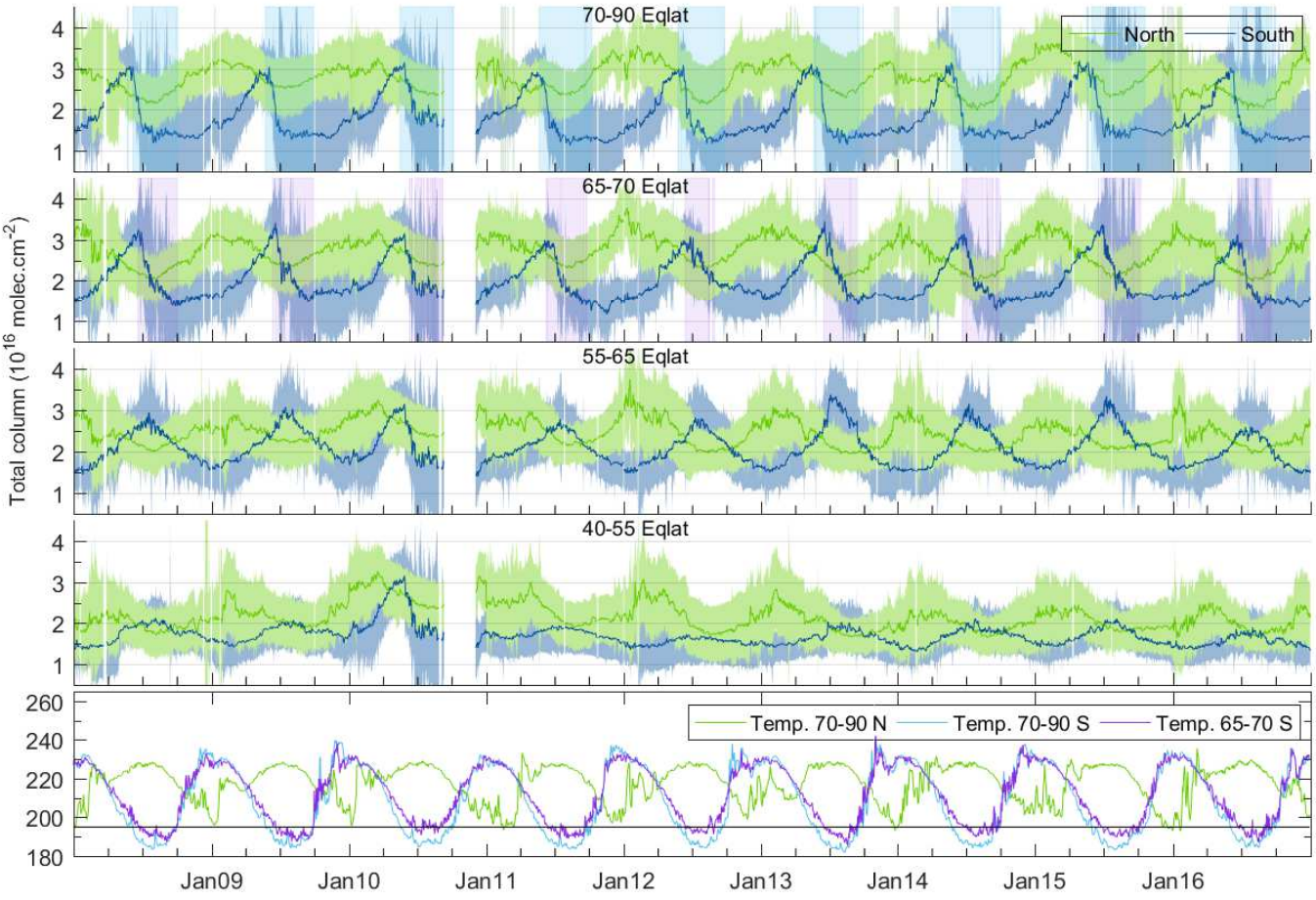

Figure 2. ~~(four~~ Four top panels~~)~~: HNO_3 total columns time series for the years 2008-2016, for equivalent latitude bands 70-90, 65-70, 55-65 and 40-55, north (green) and south (blue). Vertical shaded areas are the periods during which the average temperatures are below T_{NAT} in the north (green) and south (blue) 70-90° band, and in the south (purple) 65-70° band. Note that the large period without data in 2010 is when there was a low amount of data distributed by EUMETSAT (~~bottom panel~~see Section 2)~~Temperatures~~. Bottom panel: Daily average temperatures time series (in K) taken at the altitude of 50 hPa for the equivalent latitude bands 70-90° North (green) and South (blue) and 65-70° South (purple). The horizontal black line represents T_{NAT}, i.e. the 195 K line.

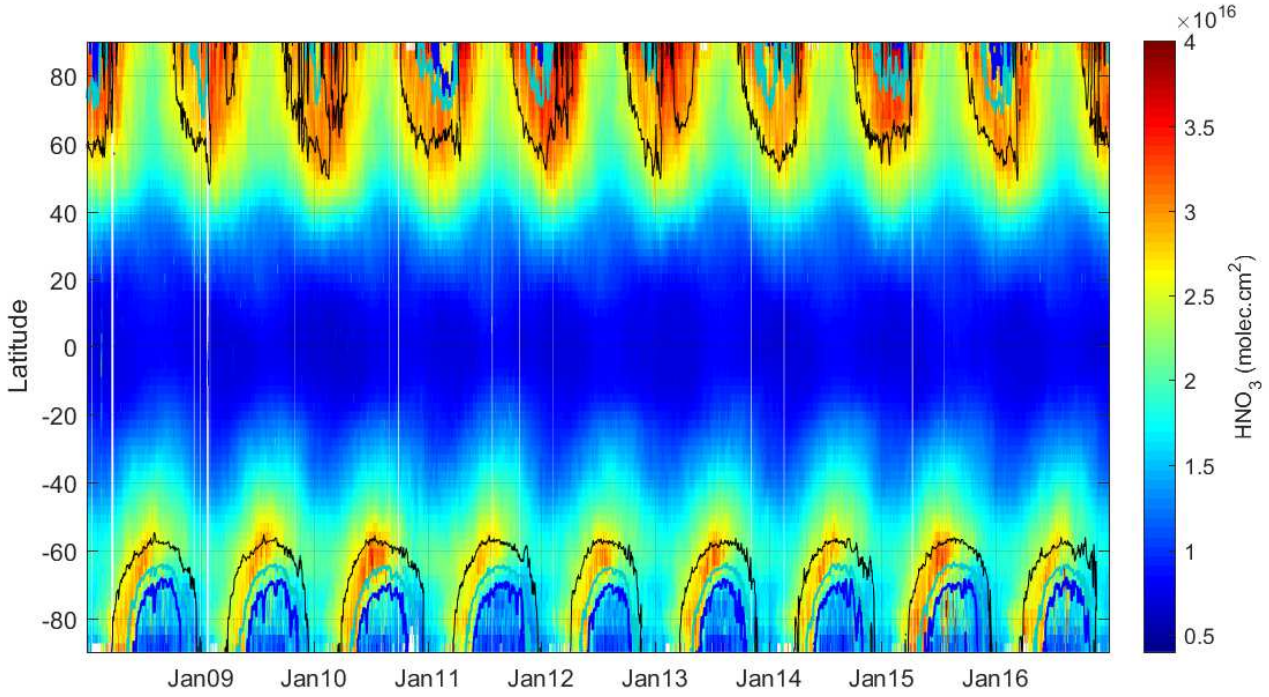

Figure 3. Zonally averaged daily HNO_3 total columns distribution over 2008-2016, expressed in molec.cm^{-2}. The lines represent potential vorticity contours at a potential temperature of 530 K (5 (black), 8 (cyan) and 10 (blue)$\times 10^{-6}$ K.m^2.kg^{-1}.s^{-1}) which correspond to the equivalent latitudes contours illustrated in Fig 1.

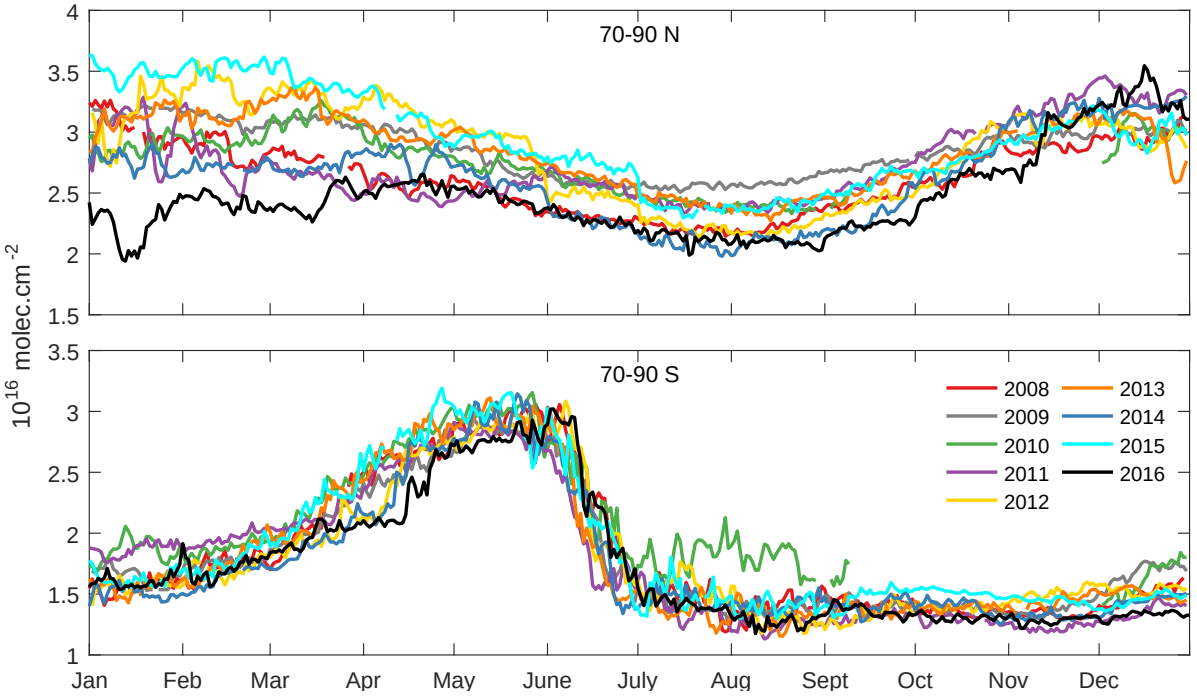

Figure 4. For northern (top) and southern (bottom) 70-90 equivalent latitude bands: HNO_3 total columns time series for the years 2008 to 2016 in molec.cm^{-2}. Note that the y-axis limits differ between the two plots.

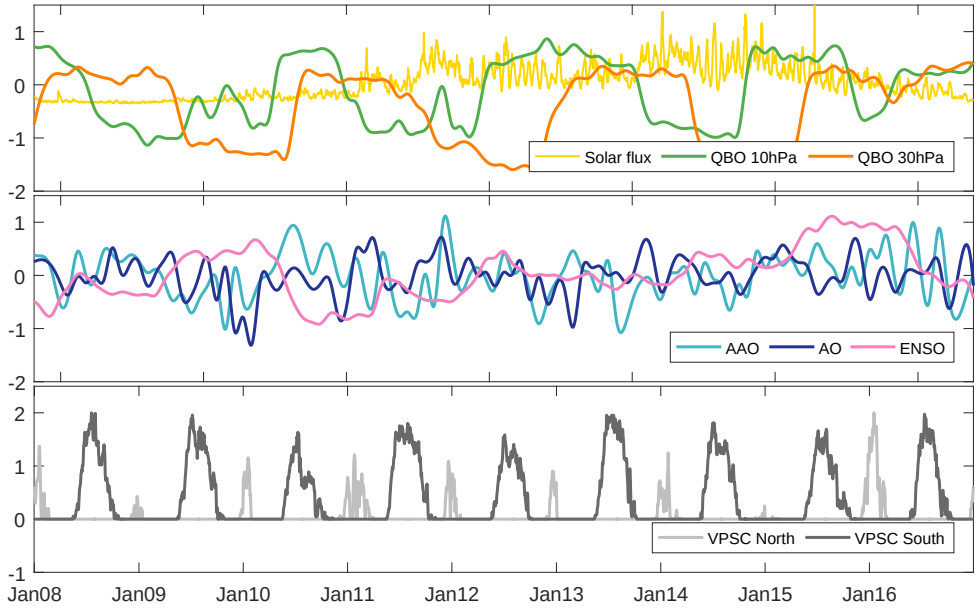

Figure 5. Normalized proxies over the IASI observations period (2008-2016). ~~(top~~ Top panel~~):~~ Solar flux (yellow), QBO at 10 hPa (green) and QBO at 30 hPa (orange). ~~(middle~~ Middle panel~~):~~ Antarctic Oscillation (light blue), Arctic oscillation (dark blue) and Multivariate ENSO Index (MEI, pink). ~~(bottom~~ Bottom panel~~):~~ VPSC proxy in the northern hemisphere (light grey) and in the southern hemisphere (dark grey).

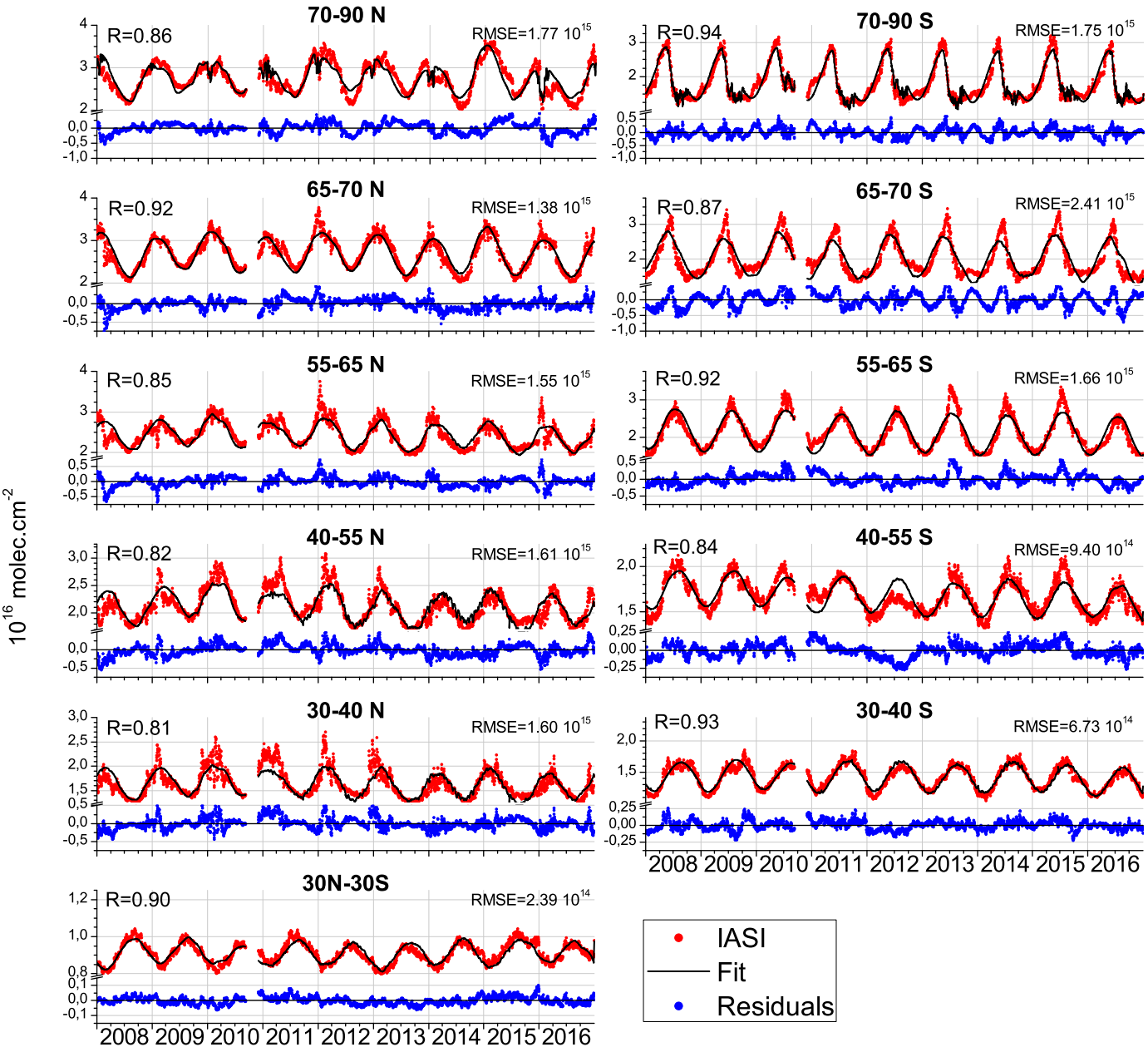

Figure 6. IASI HNO_3 total columns (red dots) for each equivalent latitude bands and the associated fitted model (black curves). The residuals are in blue, and the horizontal black line represents the zero residual line. For each equivalent latitude band, the correlation coefficient (R) between the observations and the model fit is given in the top left corner, and the root mean square error (RMSE) in the top right corner.

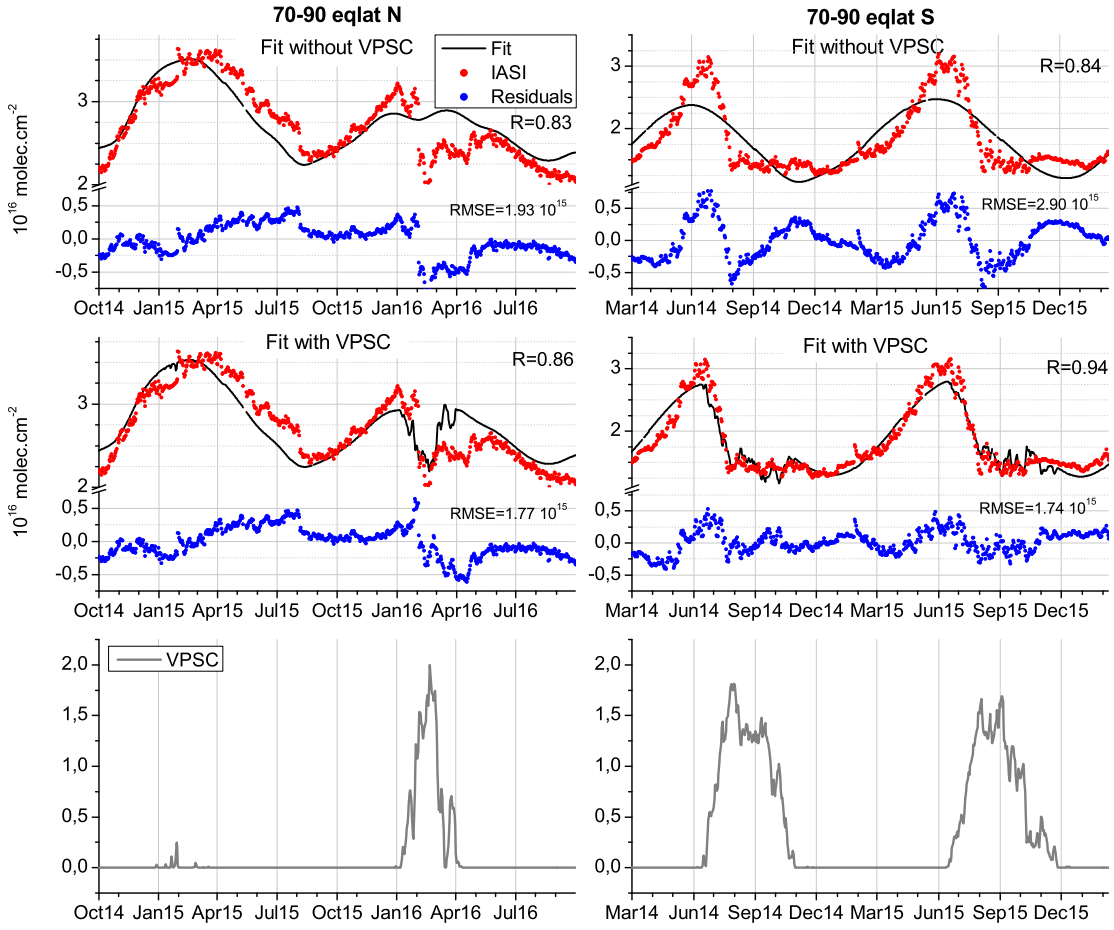

Figure 7. For north (left) and south (right) equivalent latitude bands 70-90°: ~~(top)~~ Top: Total columns (in 10^{16} molec.cm^{-2}) of IASI observations (red) and the regression fit without the VPSC proxy (black), for a subset of the time series, zooming on denitrification periods. The correlation coefficients between the fit and the IASI data (R) are displayed, as well as the root mean square error (RMSE). ~~(middle)~~ Middle: Same as top panels but for the fit with the VPSC proxy. ~~(bottom)~~ Bottom: Normalized VPSC proxy. Note the different time and value ranges between the two hemispheres.

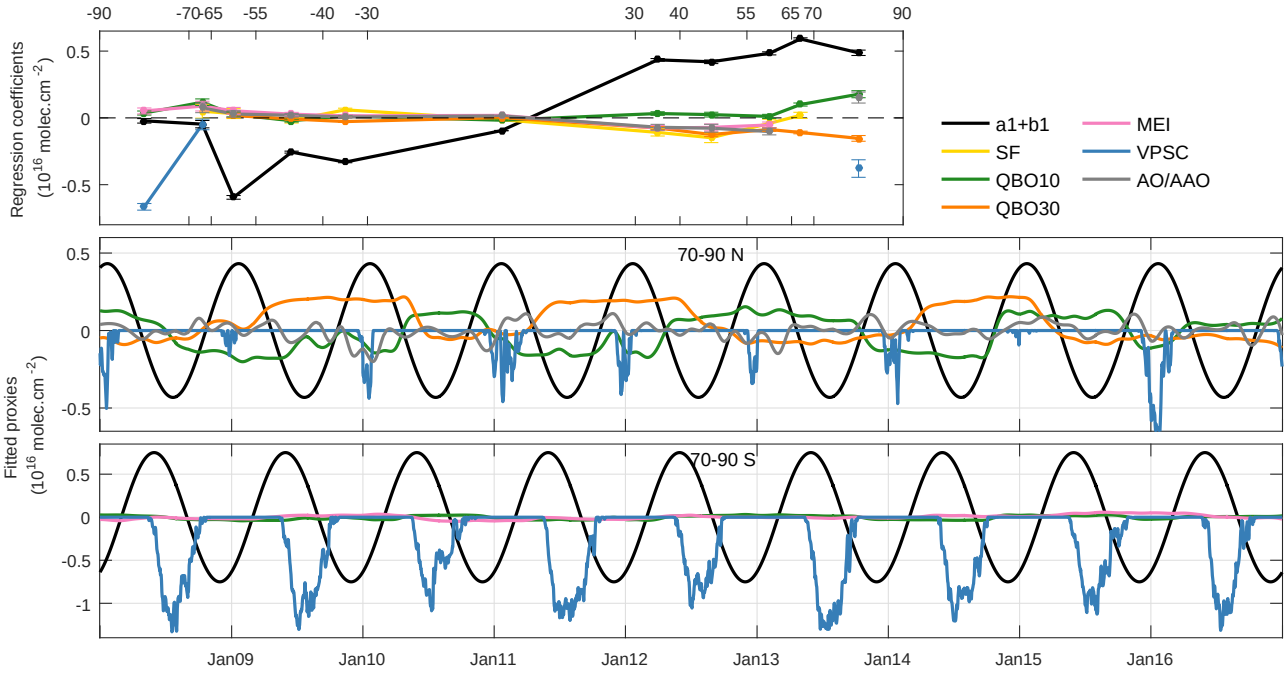

Figure 8. ~~(top~~ Top panel~~)~~: Regression coefficients (x_i) and their standard error (σ_e, error bars, calculated by Eq. 3) for the selected variables in each equivalent latitude band (each data point is located in the middle of its corresponding eqlat band). ~~(bottom~~ Bottom panels~~)~~: Fitted signal of the proxies in the eqlat bands 70-90 north (middle) and south (bottom) for the variables selected. They are calculated as $[x_i.X_i]$ with X_i the normalized proxy and x_i the regression coefficient calculated by the regression model.

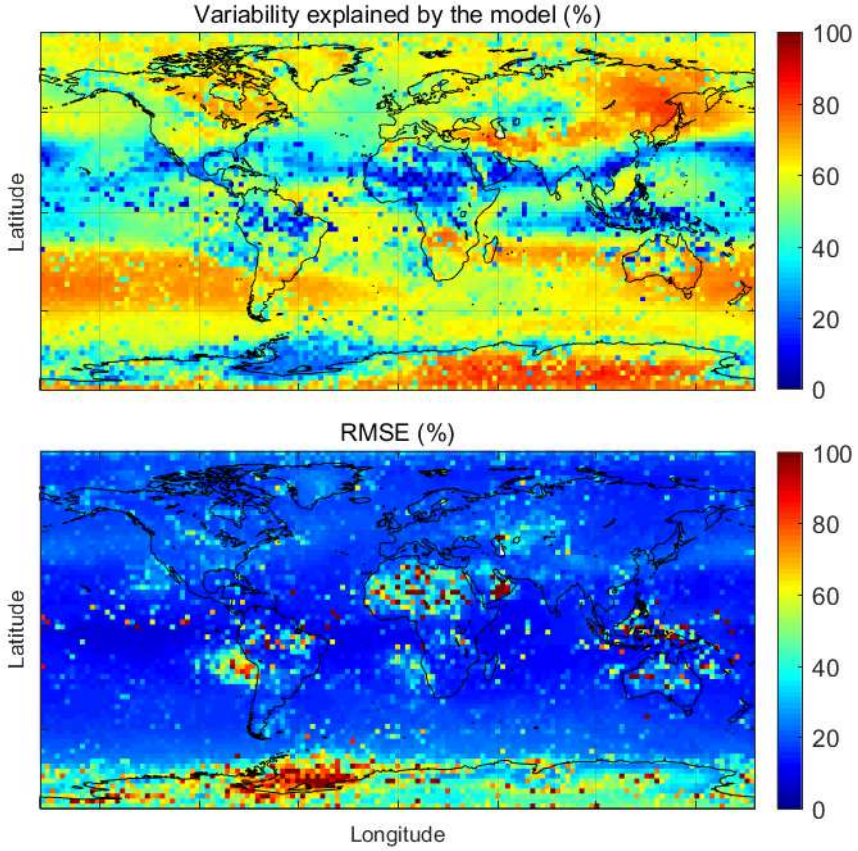

Figure 9. ~~(top)~~ Top: Fraction (%) of the HNO_3 variability in the IASI observations explained by the regression model, and calculated as $[\sigma(HNO_3{}^{\text{fit}})/\sigma(HNO_3{}^{\text{IASI}}) \times 100]$. ~~(bottom)~~ Bottom: Root Mean Square Error (RMSE) calculated for each grid cell as $[\sqrt{\frac{\sum(\text{fit-IASI})^2}{n}}]$ and expressed in %.

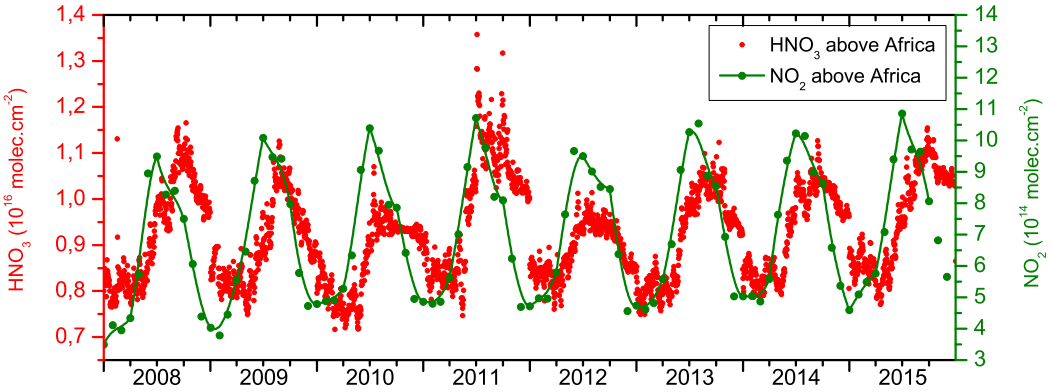

Figure 10. Time evolution of IASI HNO_3 (red) and GOME-2 NO_2 (green) from 2008 to 2015 for Africa south of the equator (5-20°S, 10-40°E). Both HNO_3 and NO_2 columns are expressed in molec.cm^{-2}. The NO_2 data are tropospheric columns (Valks et al., 2011) and are obtained from ftp://atmos.caf.dlr.de/. Note that the ranges differ between the two y-axes.

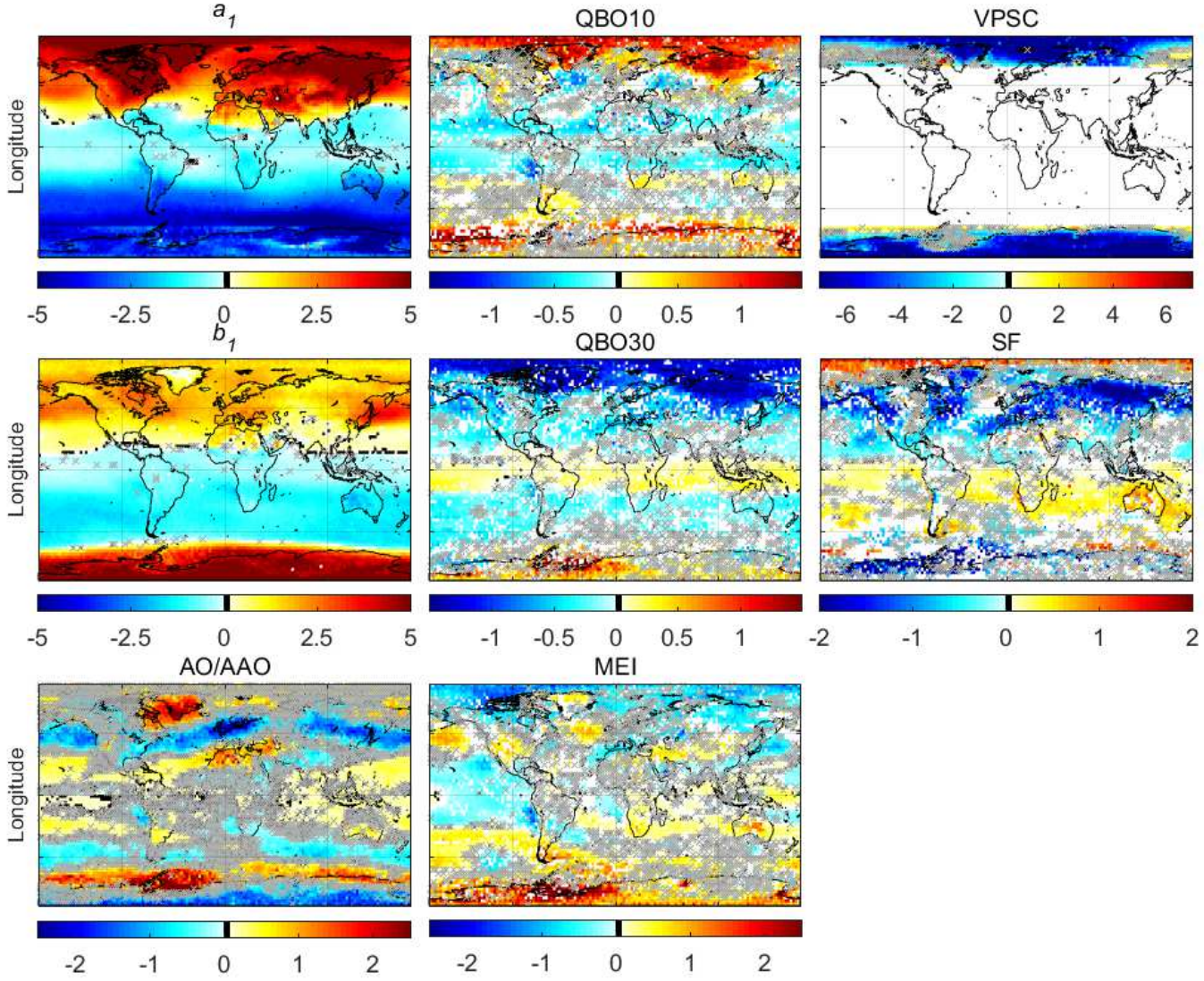

Figure 11. Global distributions ($2.5^\circ \times 2.5^\circ$ grid) of the regression coefficients expressed in 10^{15} molec.cm^{-2}. The gray crosses are the cells where the proxy is not significant when accounting for autocorrelation (see Eq.3). The white cells are where the proxy was not retained and the black cells represent a coefficient of 0. Note the different scales. The X axes are latitudes.